

Supporting Information

A One-Dimensional Fluidic Nanogenerator with a High Power Conversion Efficiency

*Yifan Xu⁺, Peining Chen⁺, Jing Zhang, Songlin Xie, Fang Wan, Jue Deng, Xunliang Cheng, Yajie Hu, Meng Liao, Bingjie Wang, Xuemei Sun, and Huisheng Peng**

anie_201706620_sm_miscellaneous_information.pdf

anie_201706620_sm_Movie_S1.mp4

Supporting Information

Experimental Section

Preparation of the FFNG. A rubber fiber with a diameter of 0.8 mm was wrapped by an aligned MWCNT sheet with a width of 0.9 cm drawn from a spinnable MWCNT array synthesized by chemical vapour deposition. The wrapping process was repeated twice for each fiber and an MWCNT-sheet-thickness of ~260 nm was achieved. To fabricate the stretchable FFNG, the substrate was changed to a pre-stretched elastic rubber fiber. After wrapping one layer of the aligned MWCNT sheet on the rubber fiber, the resulting composite fiber was dipped into a dispersion of OMC particles (CMK-3, Nanjing XFNANO Materials Tech Co.) in ethanol. The OMC-incorporated FFNG was obtained by evaporation of ethanol, followed by wrapping another layer of MWCNT sheet. The OMC content between two neighbouring MWCNT sheets was normalized to the length of the FFNG, and could be easily controlled. The OMC contents were increased from 0 to 10.2 $\mu\text{g}/\text{cm}$ by increasing the concentration of the OMC dispersion from 0 to 8 mg/mL.

Measurements for electricity generation. Copper wires were used to connect the two ends of an FFNG for measurement. During a flowing test, the FFNG was first placed at the centre of a plastic tube (1.5 mm in diameter). The saline water was then injected into the tube from one end by a programmable syringe pump (TJ-3A, Longer Pump) that could control the flowing velocity. The other end was prevented from touching the saline water. During the stretching test, an elastic FFNG was half-submerged in the saline water. It was studied with one end fixed at the bottom and the other being pulled at different frequencies. The output voltage and current between two ends were recorded at a Keithley Model 2400 Source Meter. For the blood flow detection, a 10-cm-long FFNG was fixed in a tube to detect the blood flowing velocity through the flowing potential. For the nerve stimulation, three 10-cm-long OMC-incorporated FFNGs were assembled in plastic tubes and connected in series to stimulate the sciatic nerve of a frog. An HY0350 Table-top Universal Testing Instrument was used to record the tension generation of the gastrocnemius muscle.

Characterization. The structures were characterized by scanning electron microscopy

(Hitachi FE-SEM S-4800 operated at 1 kV) and transmission electron microscopy (JEOL JEM-2100F operated at 200 kV). The photographs were taken by a camera (Nikon, J1). The resistance variation under stretching was recorded by the Keithley Model 2400 Source Meter. The cyclic voltammograms were measured through an electrochemical work station (CHI 660D). The I-V curves of the CNT in deionized water and 0.6 M NaCl were also measured through the electrochemical work station (CHI 660D). The current and power densities were normalized to the surface area covered with MWCNTs in the FFNG and the mass of the electrode (MWCNTs and OMC particles). The zeta potential of the CNT was measured with a Zetasizer Nano ZSE (Malvern Instruments).

Power conversion efficiency. The power conversion efficiency was defined as the ratio of the flowing electric output work of the FFNG to the flowing mechanical input work of the saline water. The electricity generation of the FFNG relied on the relative movement between the surrounding saline water and the FFNG. For an FFNG that was placed in a tube, it was the movement of the solution touching the FFNG in lengthwise direction that resulted in the electricity generation. Therefore, the power conversion efficiency was calculated by the equation expressed by $\eta = 2W/(\rho \times V \times v^2)$, where W , ρ , V and v represented the electric output work during the flowing process, the density and the volume of the NaCl solution touching the FFNG in the tube and the flow velocity (16 cm/s), respectively. The total electric output work of the FFNG was calculated by the equation expressed by $W = \int_{t_0}^{t_1} P dt = 2.9 \times 10^{-6} \text{ J}$ (Figure S16). The volume of the NaCl solution could be calculated by the equation expressed by $V = \pi(D^2 - d^2)l/4$, where D , d and l were the diameter (0.35 cm) of the tube, the diameter (0.08 cm) and the length (8 cm) of the FFNG, respectively. The volume of the NaCl solution touching the FFNG was calculated as 0.73 cm^3 . Therefore, the average power conversion efficiency of the FFNG was obtained as $\sim 23.3\%$.

Power conversion efficiency of the fiber-shaped electrostatic and triboelectric nanogenerators. The calculation of the power conversion efficiency of these fiber-shaped nanogenerators is referred to that of planar nanogenerators previously reported.^[S1-S3] The power conversion efficiency of the yarn-type photoelectric conversion device (YPCD) (length of 3 cm, width of 0.2 cm) based on electrostatic effect was calculated by the equation expressed by $\eta = P_{\text{average}}/P_{\text{input}}$. Under the light with an irradiation frequency of 0.2 Hz and an irradiated intensity of 27 mW/cm^2 , P_{input}

$= 27 \text{ mW/cm}^2 \times 3 \text{ cm} \times 0.2 \text{ cm} = 16.2 \text{ mW}$, and $P_{average} = W/\Delta t = \int_{t_0}^{t_r} I^2 R dt / \Delta t = 0.23 \text{ nW}$. Therefore, the average energy conversion efficiency of the YPCD was obtained as $\eta = 0.23 \text{ nW}/16.2 \text{ mW} = 1.4 \times 10^{-8}$. The power conversion efficiency of the coaxial triboelectric nanogenerator fiber (length of 5 cm) was calculated by the equation expressed by $\eta = P_{output}/P_{input}$. Under a periodic force external force of 25 N, $P_{input} = Fl/t = 25 \text{ N} \times 0.05 \text{ m} / 0.27 \text{ s} = 4.63 \text{ W}$, and $P_{output} = UI = 5 \text{ V} \times 240 \times 10^{-9} \text{ A} = 1.2 \times 10^{-6} \text{ W}$. Therefore, the energy conversion efficiency of the coaxial triboelectric nanogenerator fiber was obtained as $\eta = 1.2 \times 10^{-6} \text{ W} / 4.63 \text{ W} = 2.6 \times 10^{-7}$. The power conversion efficiencies of these fiber-shaped nanogenerators are lower than that of the planar ones probably because of the insufficient utilization of the active surface under external forces or stimulation owing to a curved surface of the fiber.

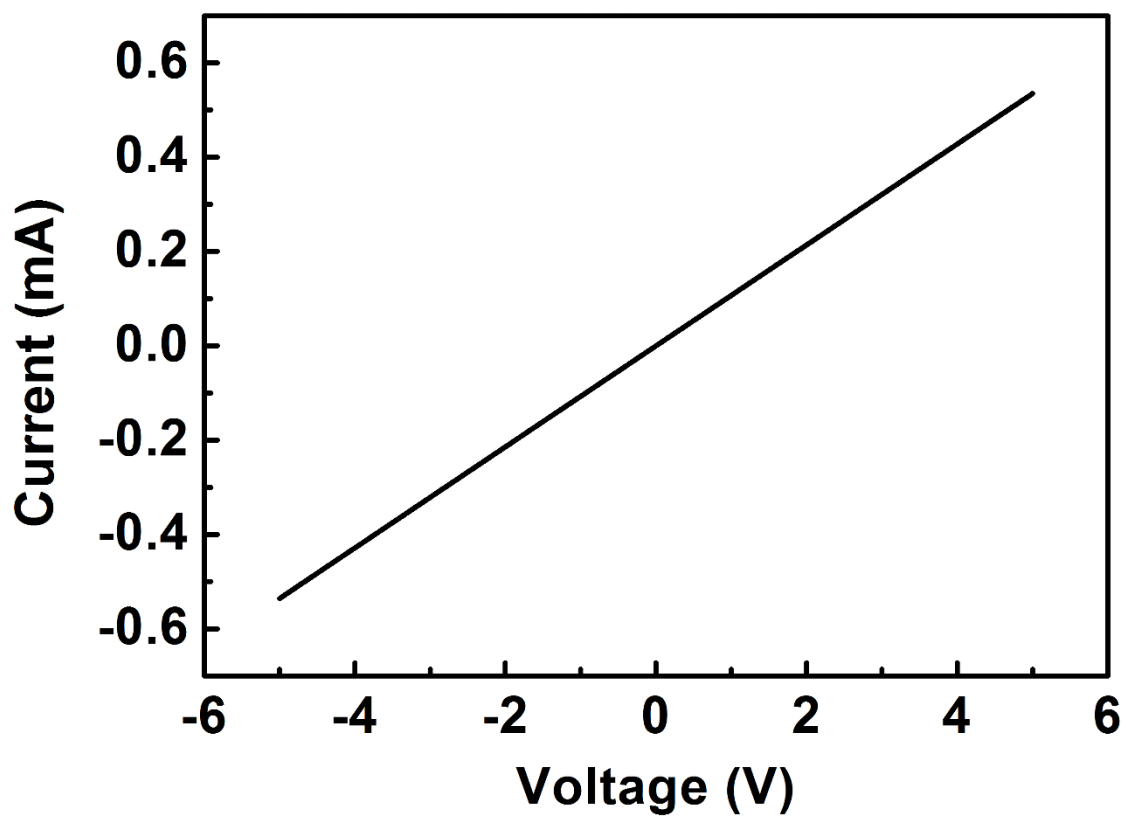


Figure S1. I-V curve of a 10-cm-long FFNG. The linearity of the curve shows a good ohmic contact.

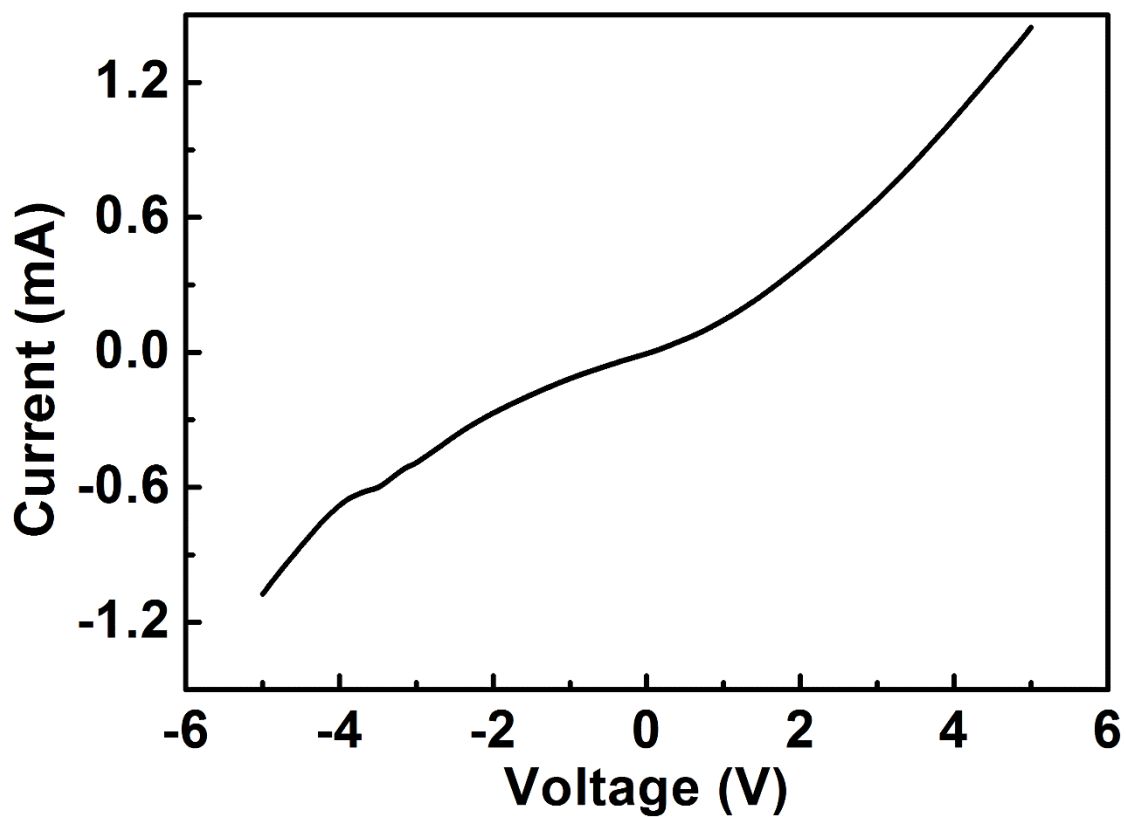


Figure S2. I-V curve of a 10-cm-long FFNG in 0.6 M NaCl. The immersed length was 8 cm. The open-circuit voltage and short-circuit current are ~ 60 mV and ~ 6 μ A, respectively.

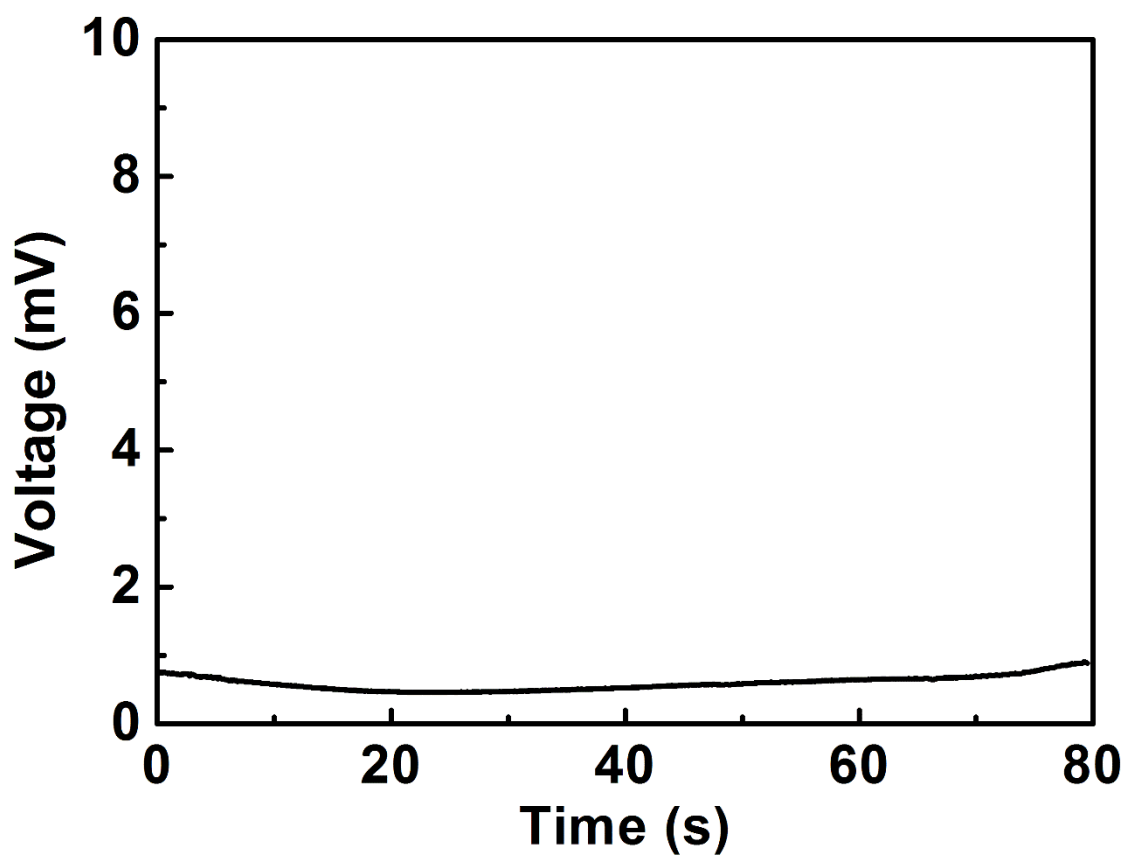


Figure S3. Output voltage of a 10-cm-long FFNG to the flow of 0.6 M NaCl solution when the whole device was immersed in the flowing saline water. The flowing velocity was maintained at 5 cm/s.

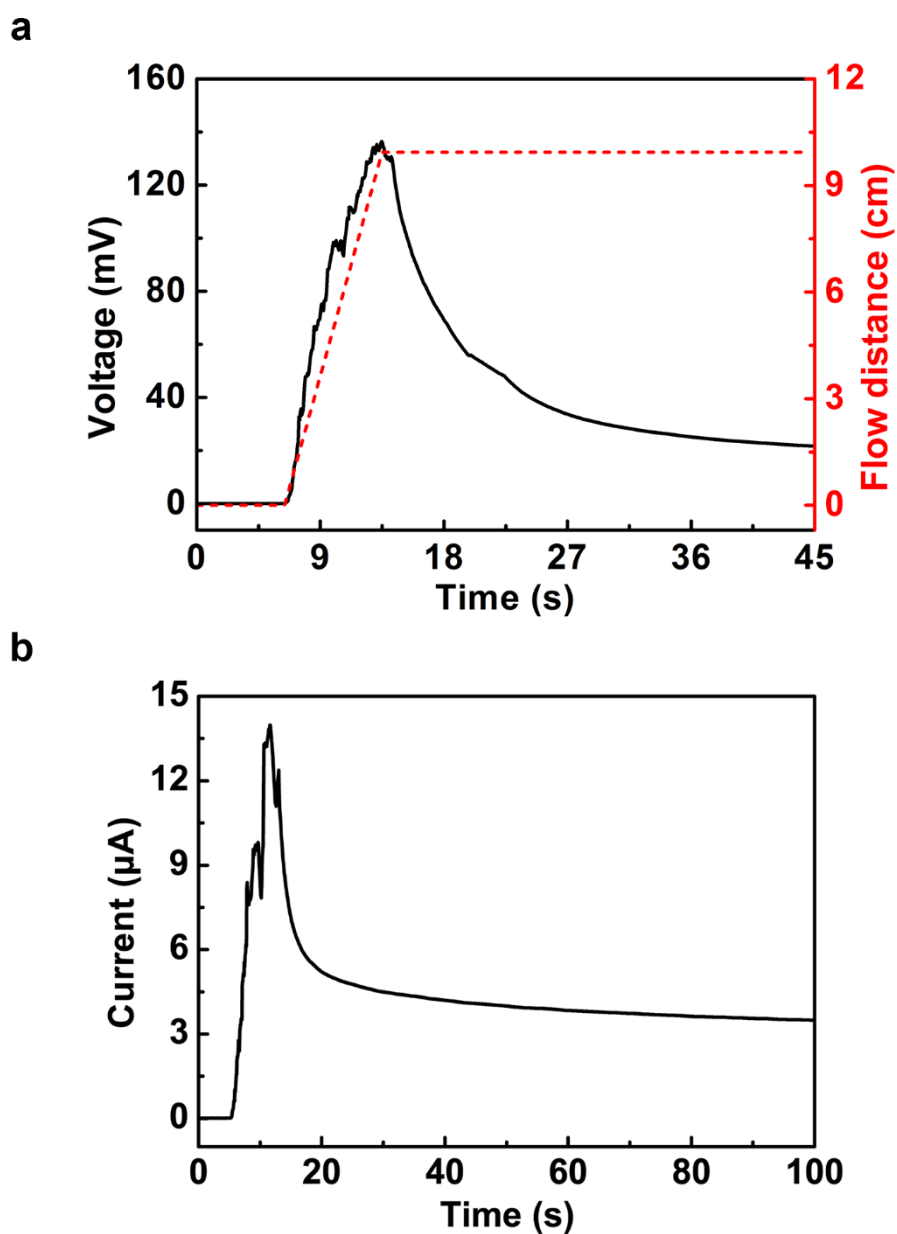


Figure S4. a) and b) Output voltage and current of an OMC-incorporated 10-cm-long FFNG to the flow of 0.6 M NaCl solution. The OMC content was 5.1 $\mu\text{g}/\text{cm}$, and the flowing velocity was 1.4 cm/s.

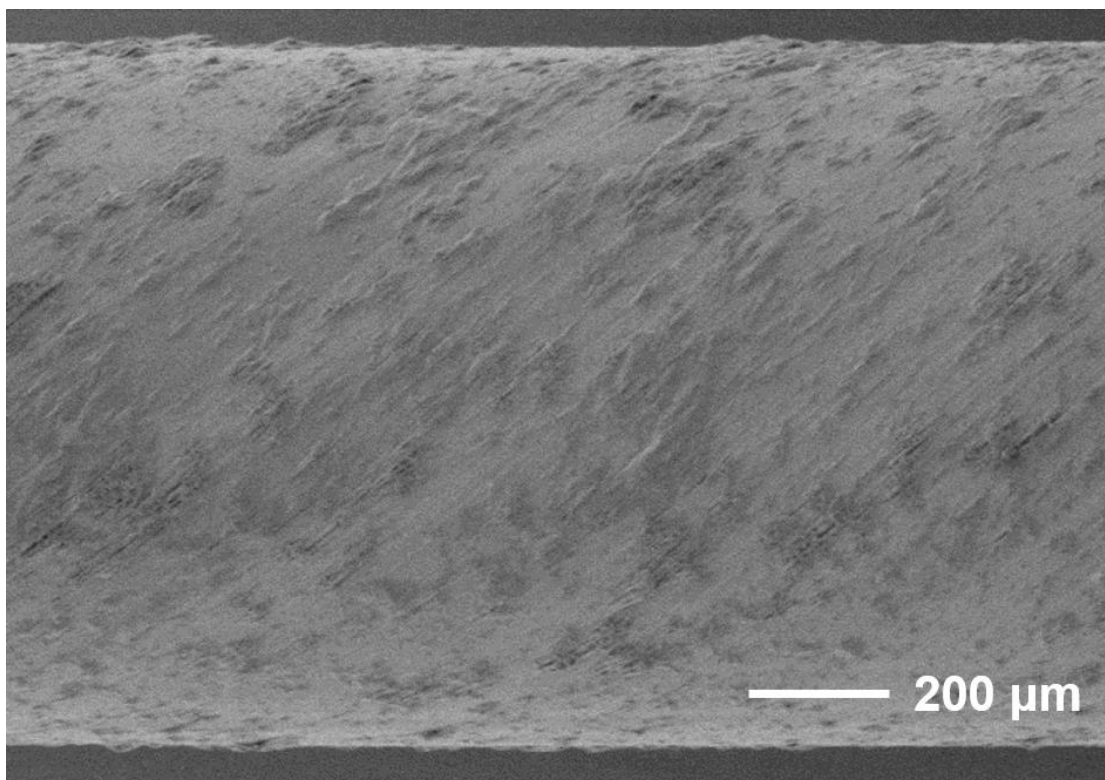


Figure S5. SEM image of the OMC-incorporated FFNG by a side view.

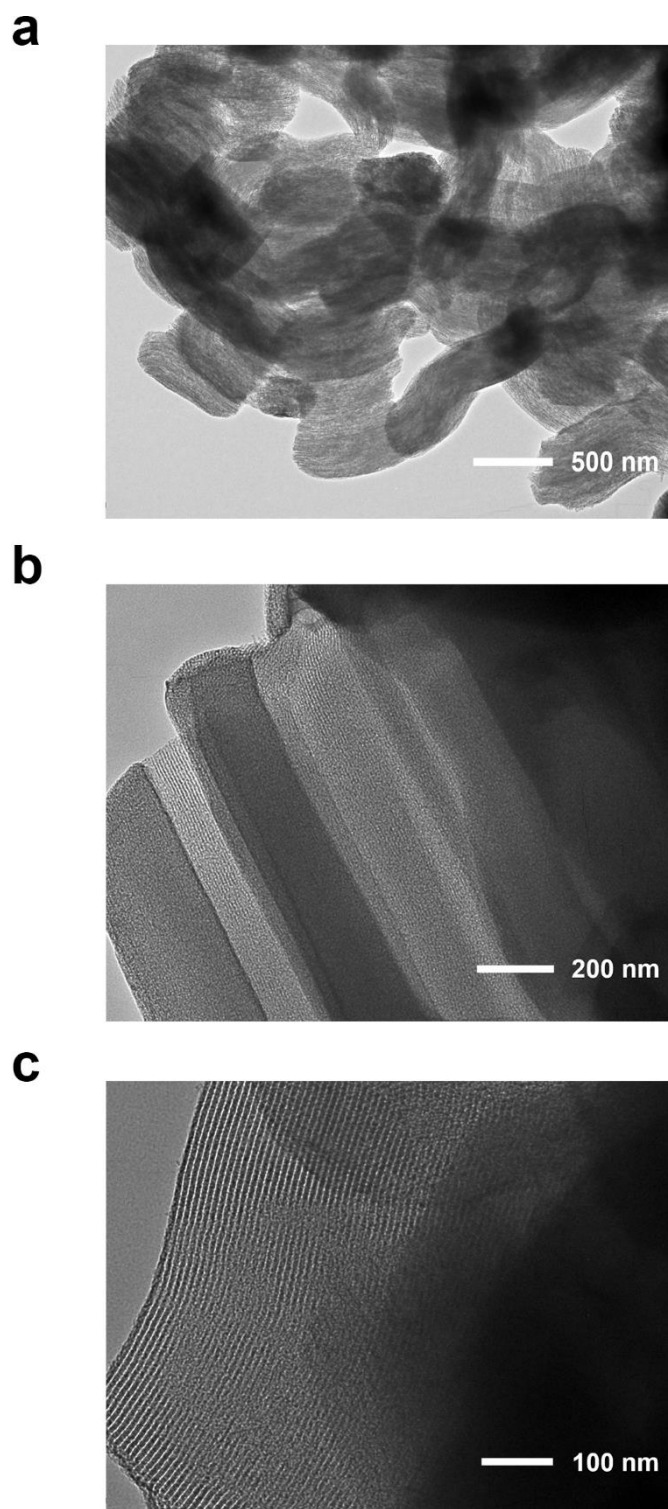


Figure S6. Transmission electron microscopy (TEM) images of the OMC particles at low and high magnifications.

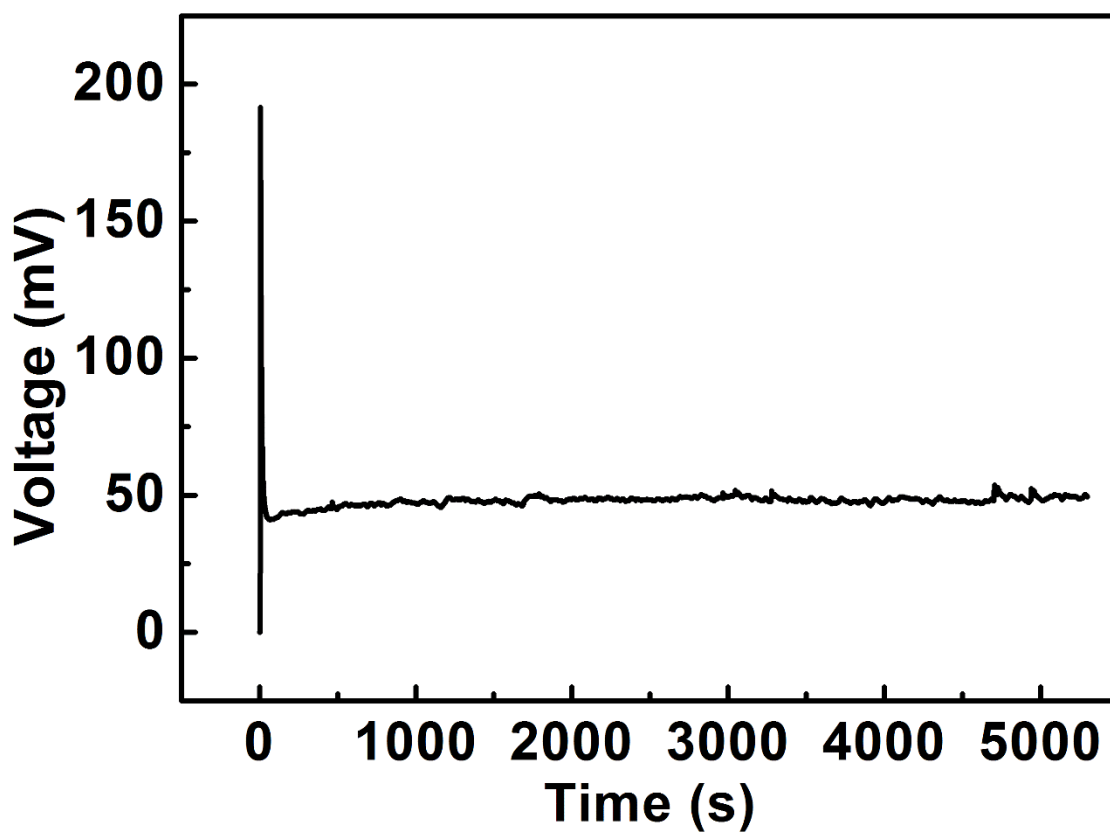


Figure S7. Output voltage of an OMC-incorporated 10-cm-long FFNG to the flow of 0.6 M NaCl solution. The OMC content was 5.1 $\mu\text{g}/\text{cm}$, and the flowing velocity was 1.4 cm/s.

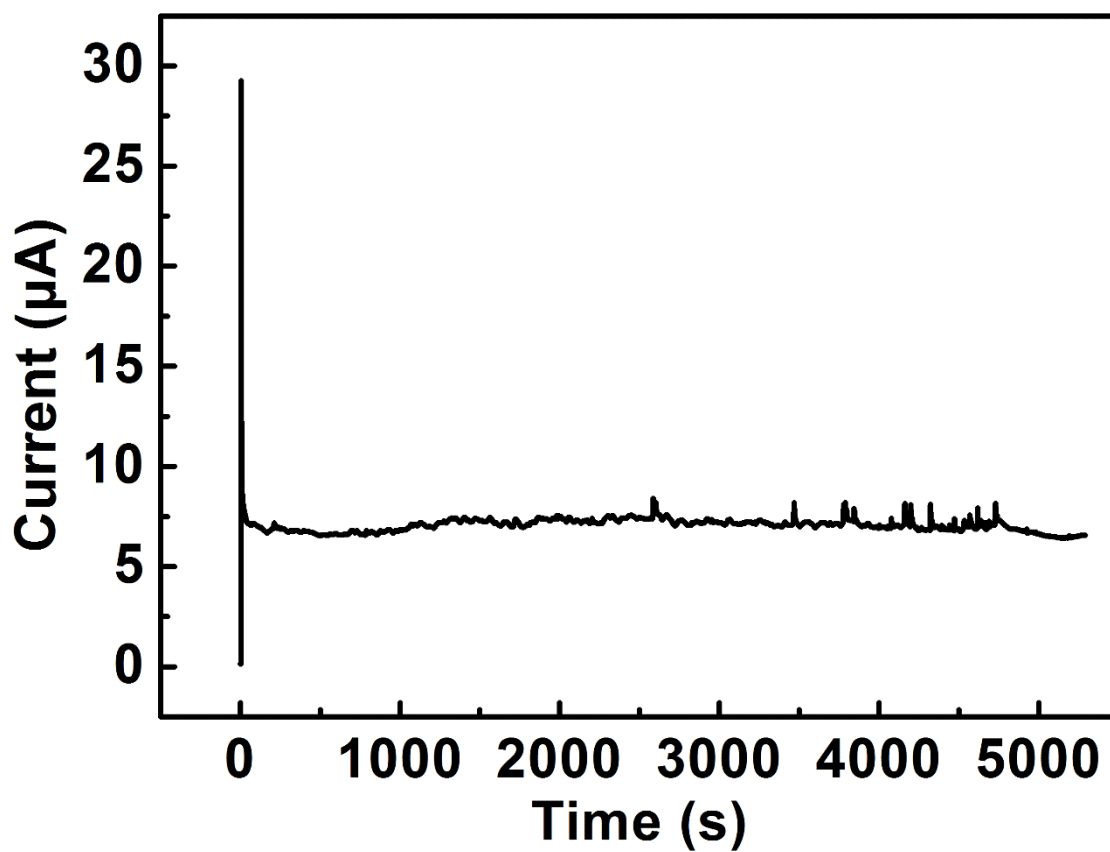


Figure S8. Output current of an OMC-incorporated 10-cm-long FFNG to the flow of 0.6 M NaCl solution. The OMC content was 5.1 µg/cm, and the flowing velocity was 1.4 cm/s.

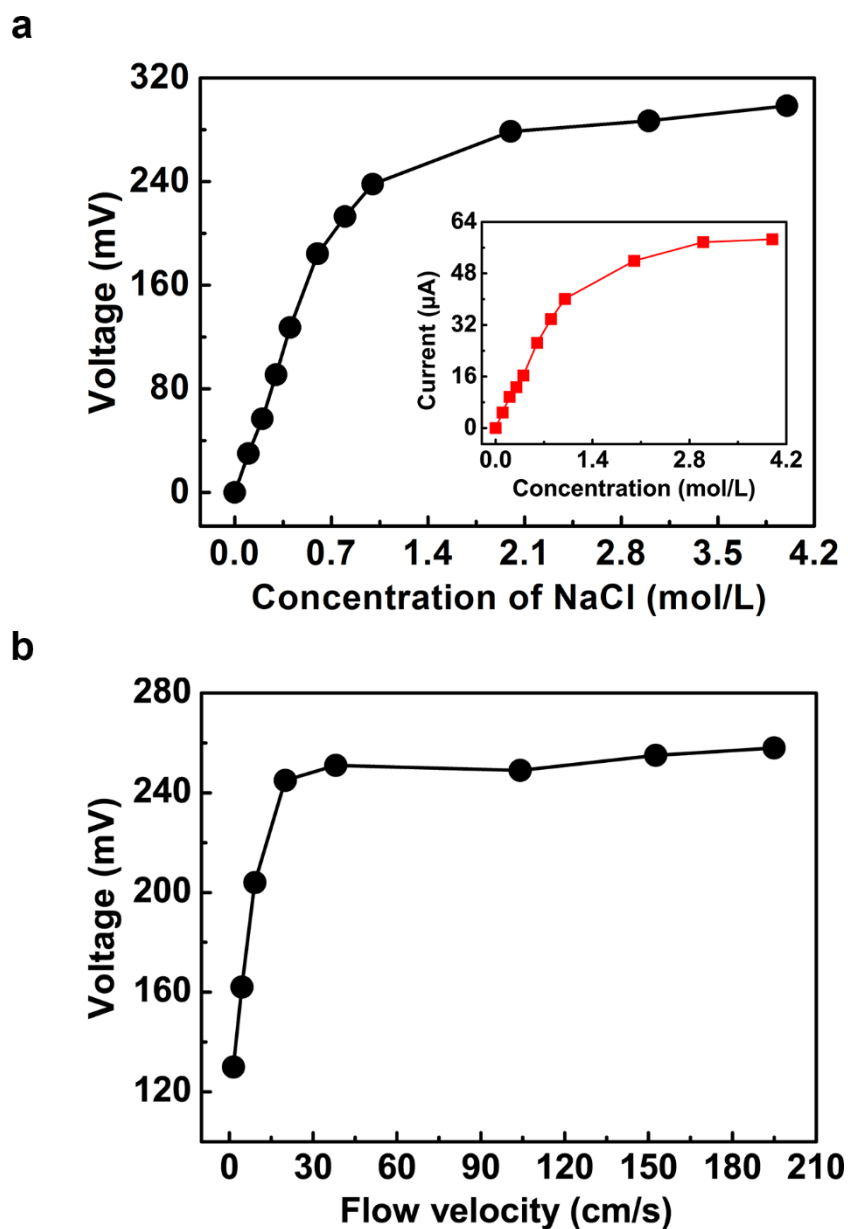


Figure S9. **a)** Dependence of output voltage of the OMC-incorporated FFNG on NaCl concentration (inserted, the corresponding output current). The flowing velocity was 9.1 cm/s. **b)** Dependence of output voltage of the OMC-incorporated FFNG on flowing velocity. The NaCl concentration was 0.6 M. For both **(a)** and **(b)**, the FFNG length and the OMC content were 10 cm and 5.1 $\mu\text{g}/\text{cm}$, respectively.

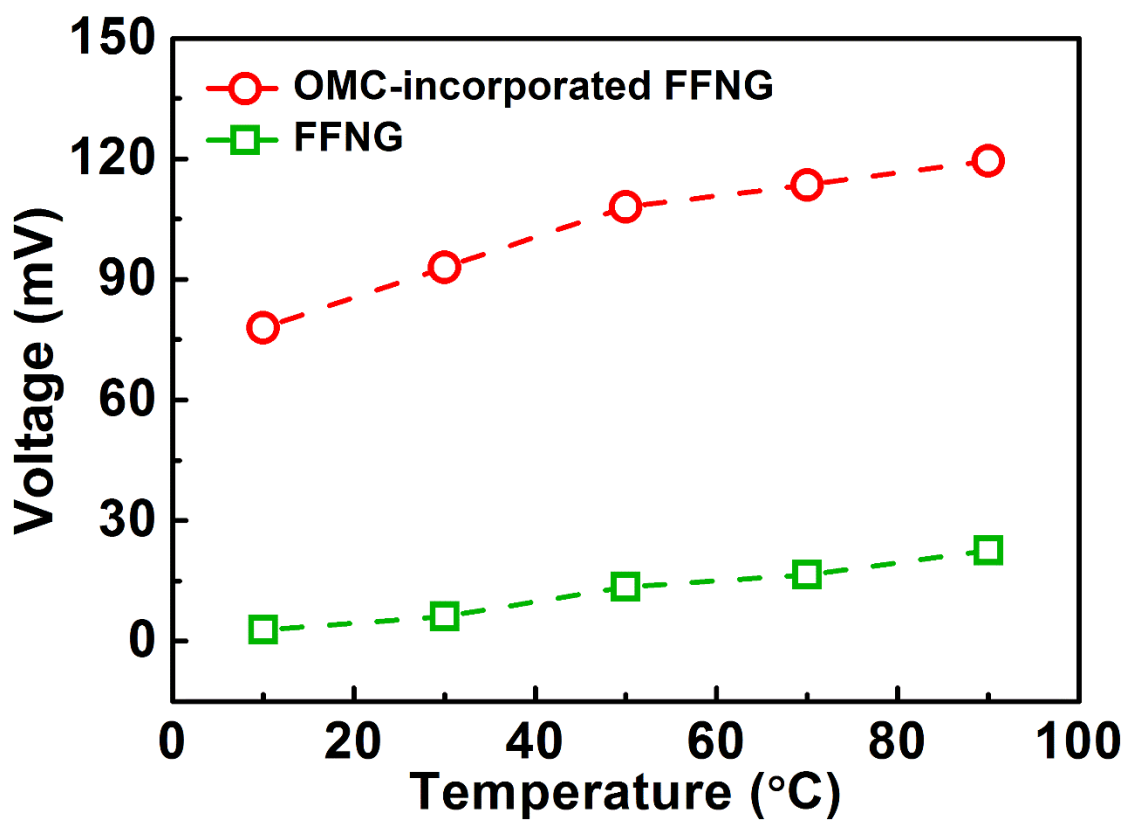


Figure S10. Dependence of output voltage on operating temperature by dipping the FFNG without and with OMC into 0.6 M NaCl solution at 16 cm/s. The total FFNG length and the immersed length were 10 and 6 cm, respectively. The OMC content was 5.1 $\mu\text{g}/\text{cm}$.

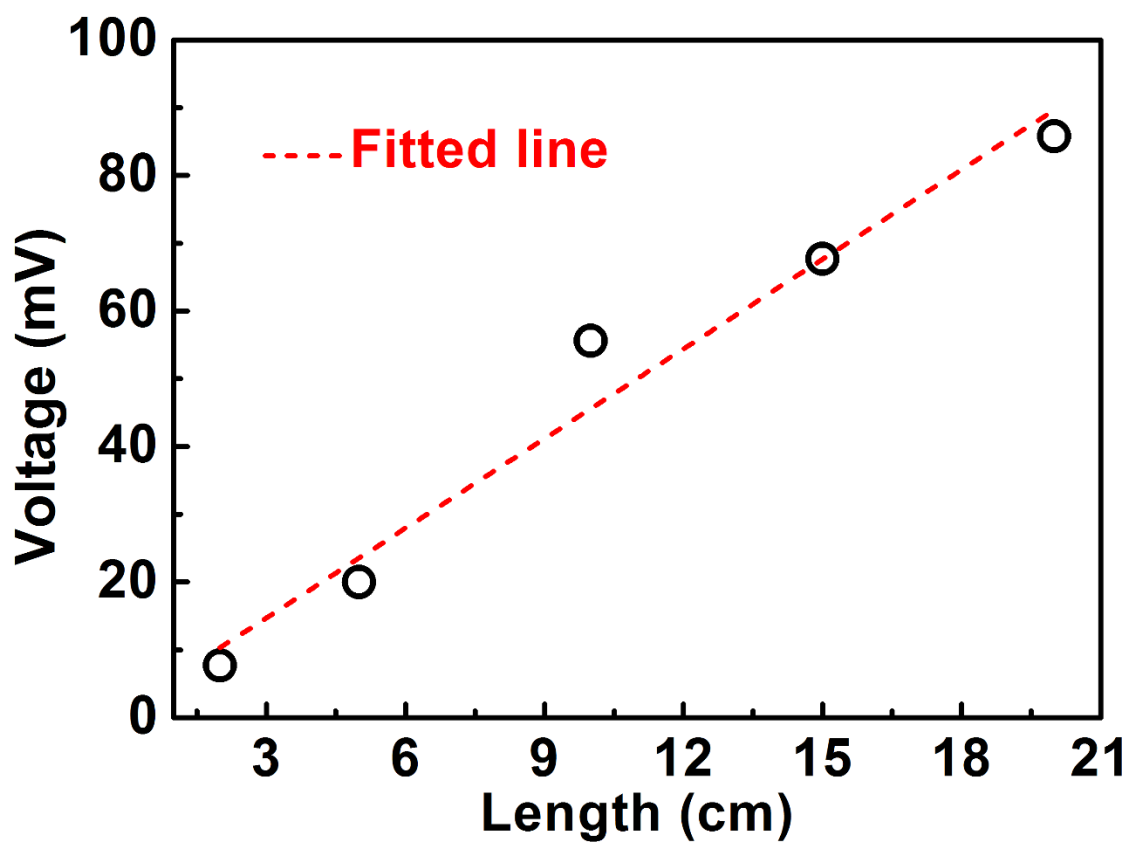


Figure S11. Dependence of the flow-induced voltage on the length of the FFNG in 0.6 M NaCl. The flowing velocity was 12.9 cm/s.

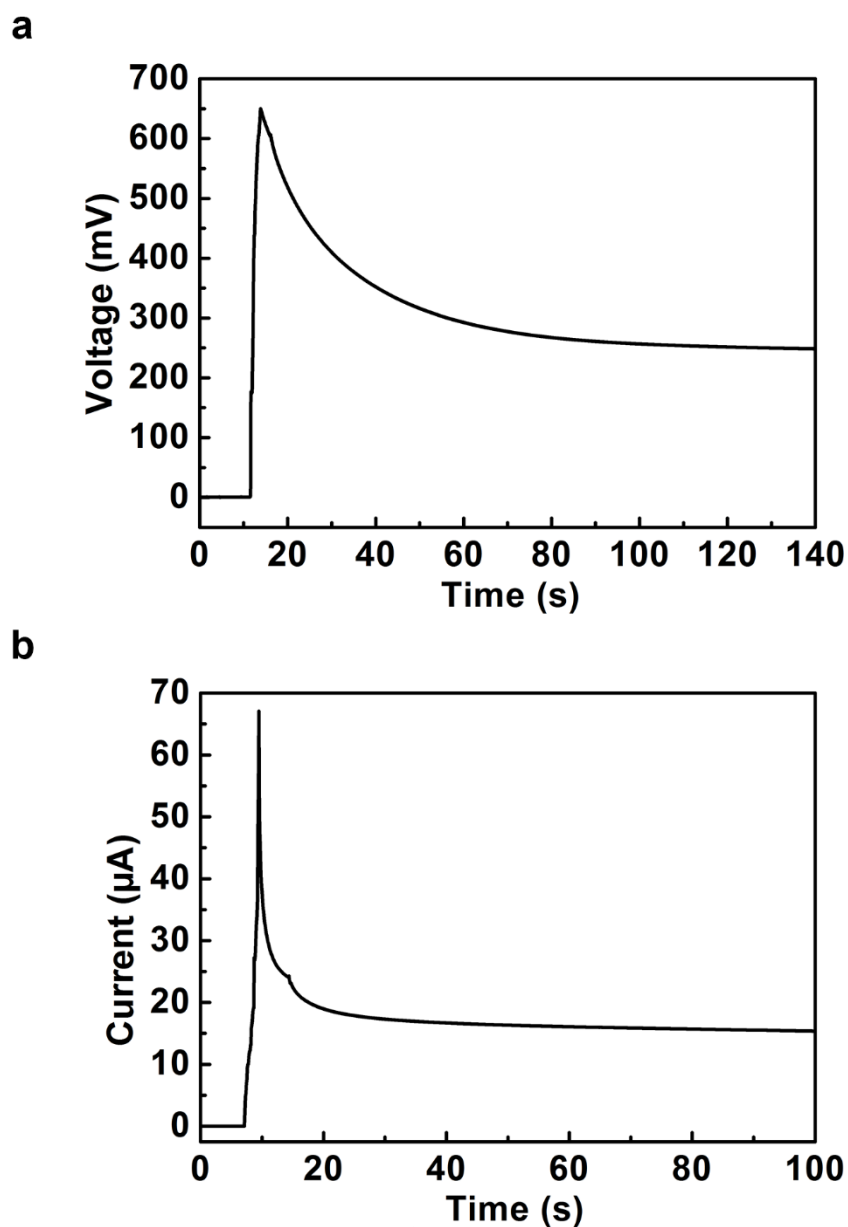


Figure S12. a) and b) Output voltage and current of a 30-cm-long OMC-incorporated FFNG in a flowing saturated NaCl solution at a velocity of 12.2 cm/s. The OMC content was 5.1 $\mu\text{g}/\text{cm}$.

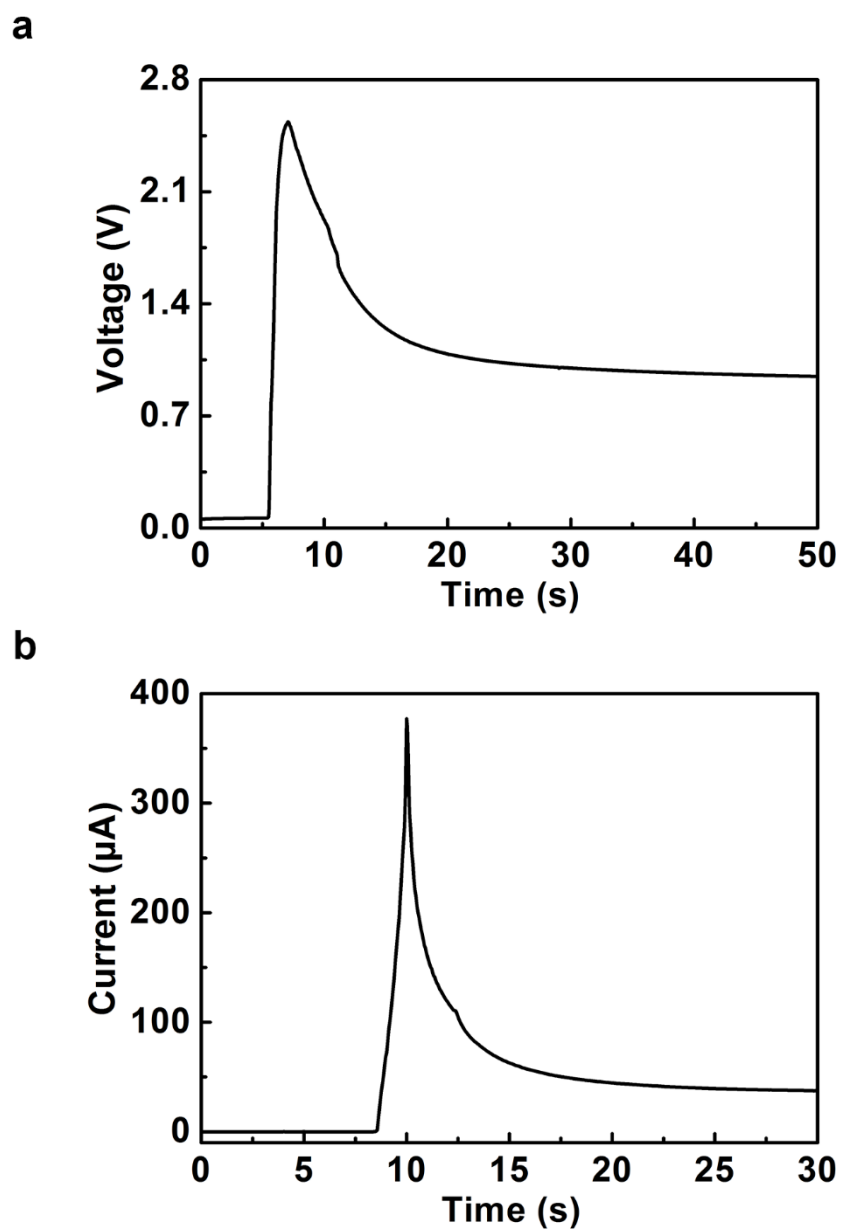


Figure S13. **a)** Output voltage of twelve 10-cm-long OMC-incorporated FFNGs connected in series. **b)** Output current of twelve 10-cm-long OMC-incorporated FFNGs connected in parallel. A saturated NaCl solution was used at both **(a)** and **(b)**.

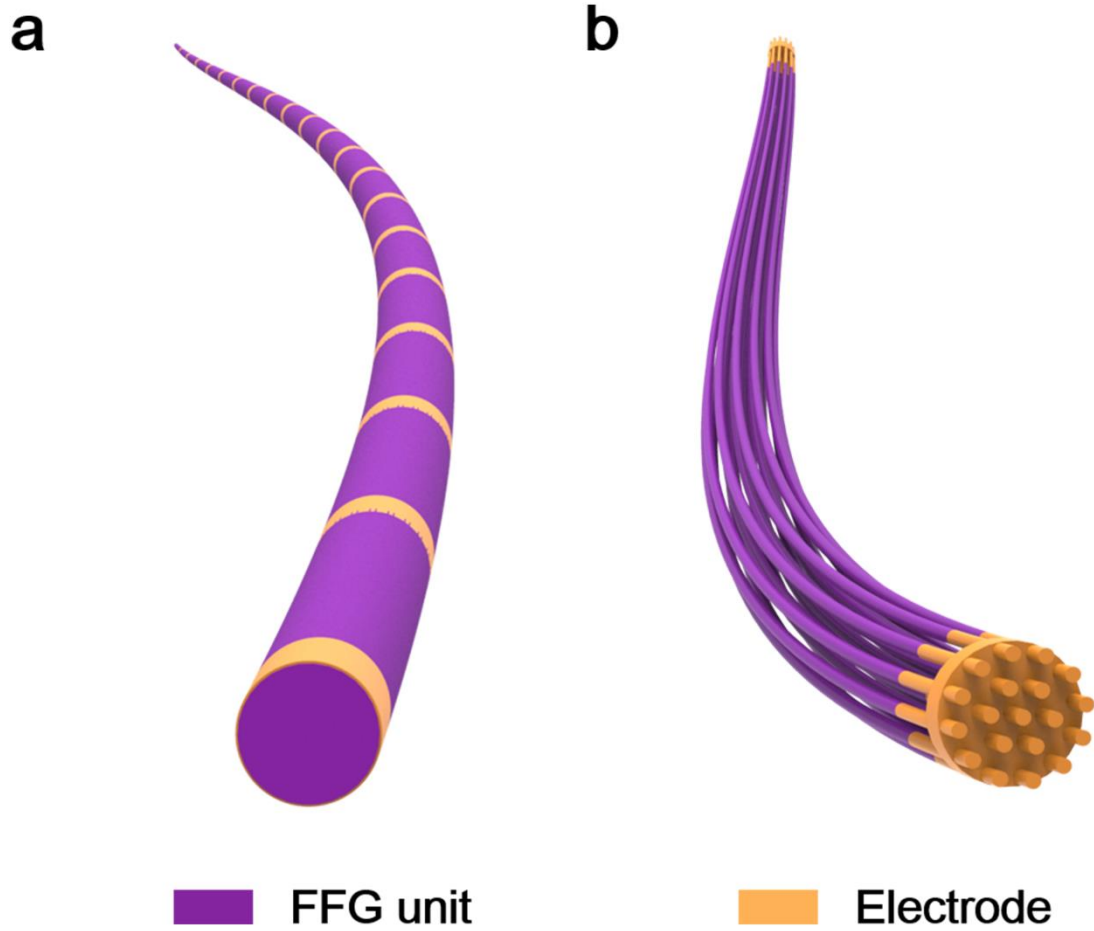
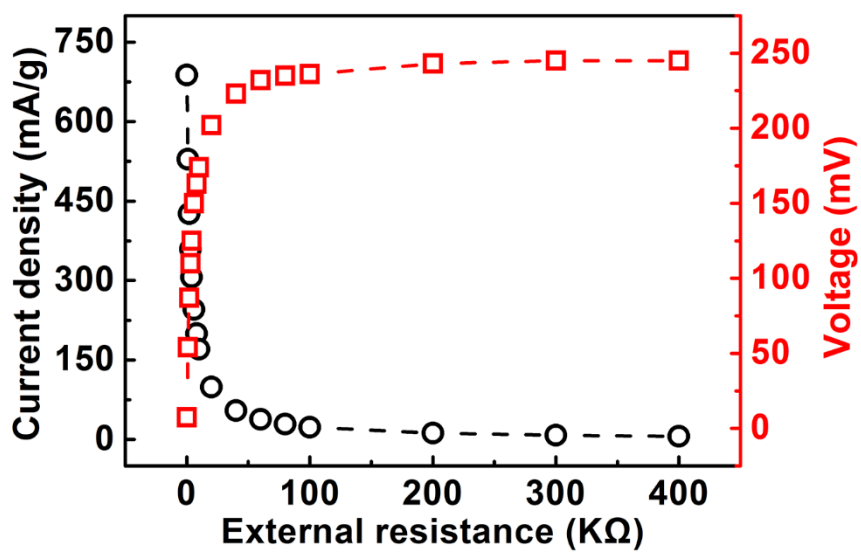


Figure S14. a) Schematic illustration to an in-series fiber-shaped energy harvesting device containing multiple FFNG units. b) Schematic illustration to an in-parallel fiber-shaped energy harvesting device containing multiple FFNG units.

a



b

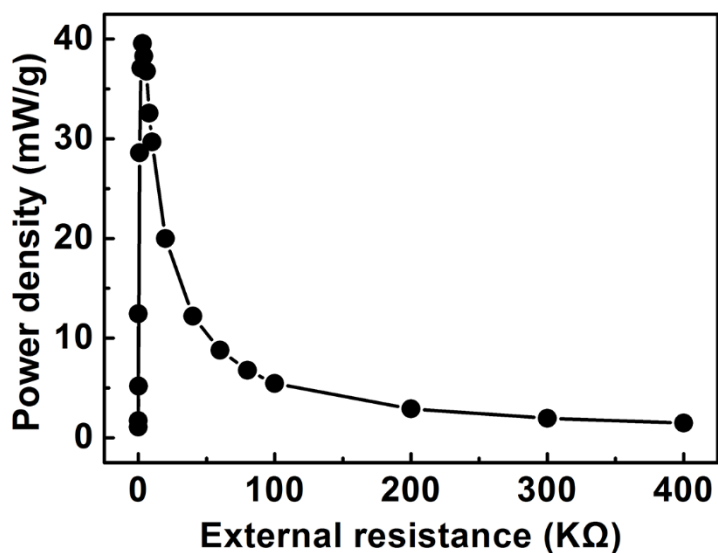


Figure S15. **a)** Dependences of current density and voltage on electrical resistance of the external circuit. **b)** Dependence of power density on electrical resistance of the external circuit. The immersed length of the OMC-incorporated FFNG (OMC content of $5.1 \mu\text{g}/\text{cm}$) was 8 cm. A saturated NaCl solution was used at both **(a)** and **(b)**.

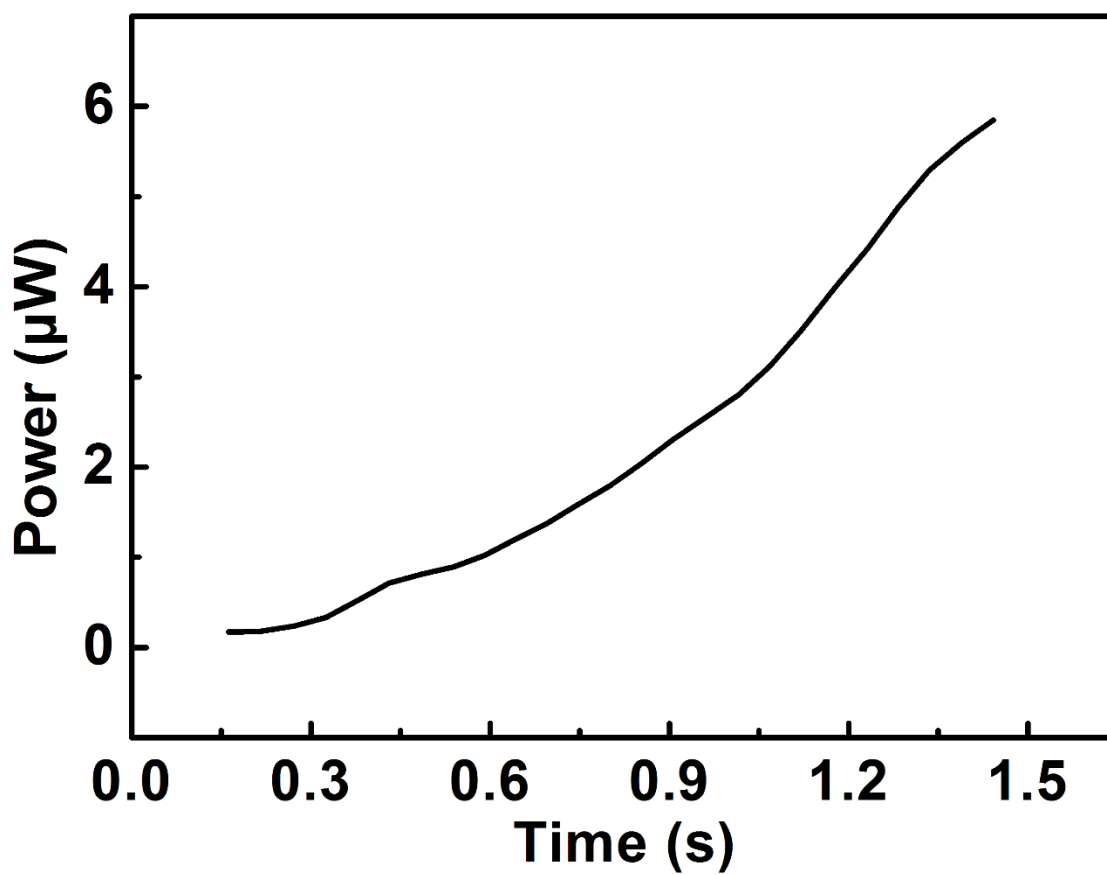


Figure S16. The power curve based on the output voltage and current of an FFNG in flowing saturated NaCl solution at an external resistance of 3 k Ω .

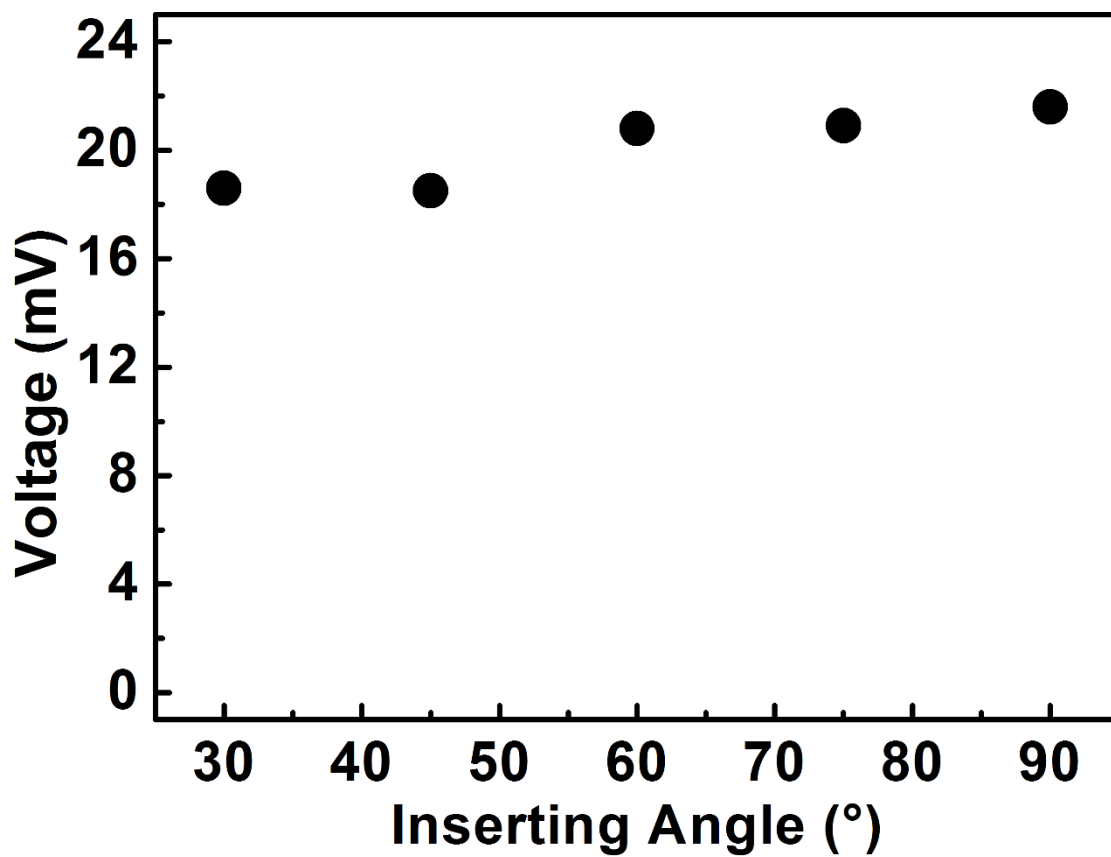


Figure S17. Dependence of output voltage on the dipping angle of the OMC-incorporated FFNG in 0.6 M NaCl solution. The immersed length of the FFNG was 1.5 cm.

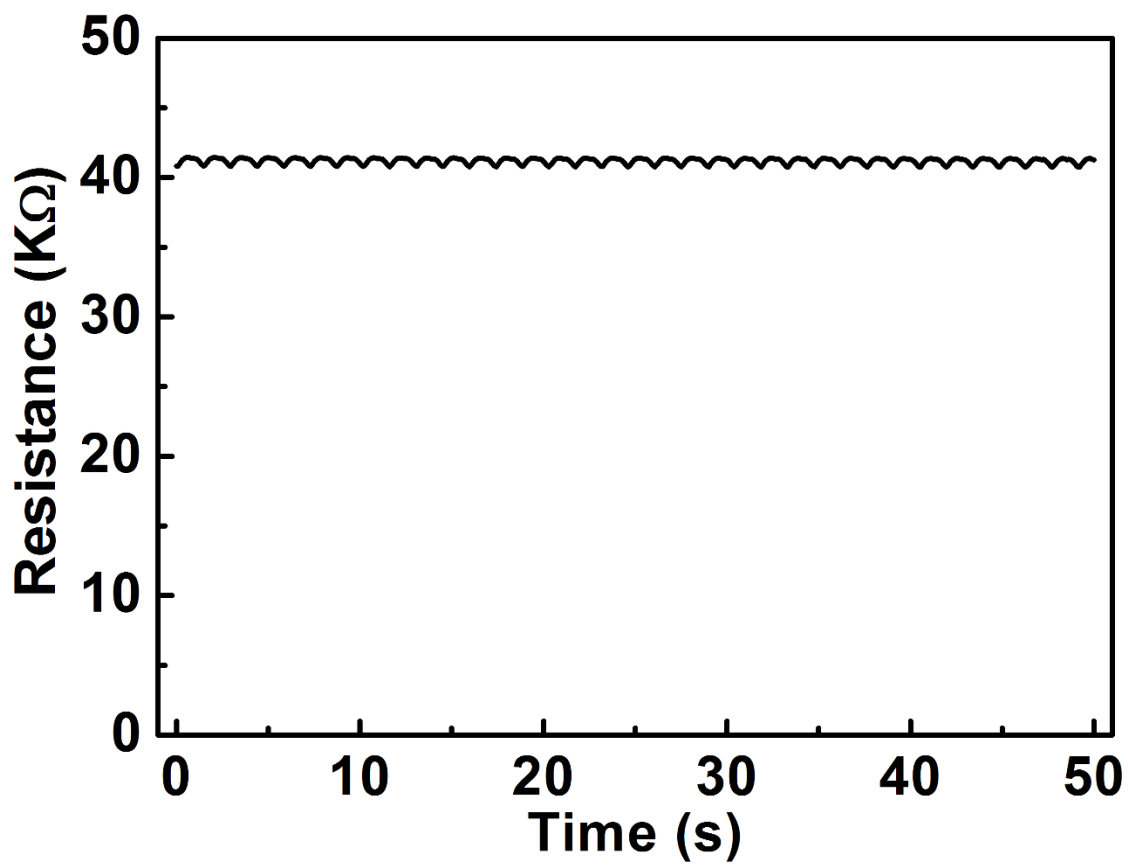


Figure S18. Resistance variation of the elastic OMC-incorporated FFNG under stretching and releasing.

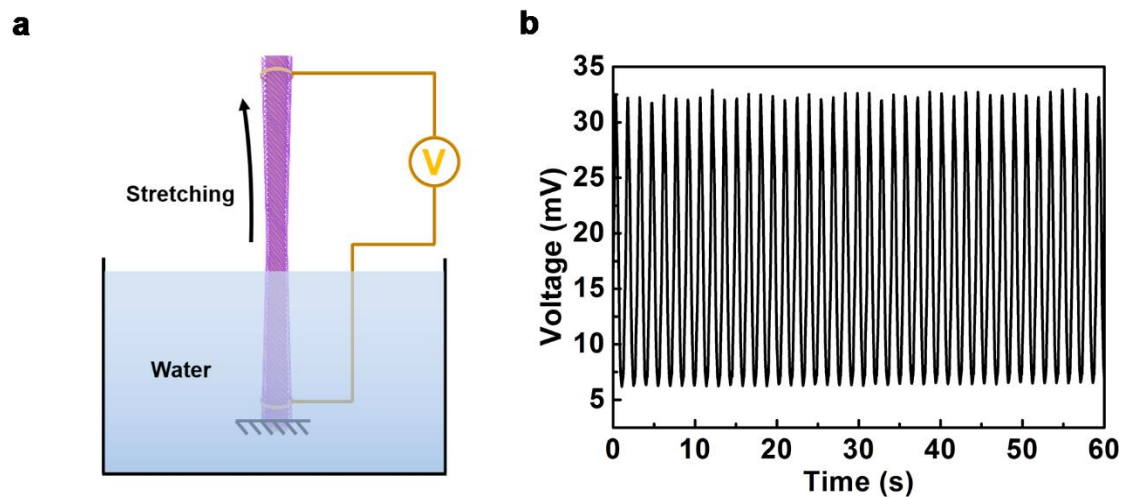


Figure S19. a) Schematic illustration to the electric output generated by stretching the elastic FFNG in a NaCl solution. The FFNG was maintained half-immersed, and the electric output was generated by pulling the FFNG end above the water level. b) Output voltage by stretching a 10-cm-long elastic FFNG to 180% with an immersed length of 5.0 cm in a saturated NaCl solution. The stretching frequency and velocity were 0.67 Hz and 10.7 cm/s, respectively.

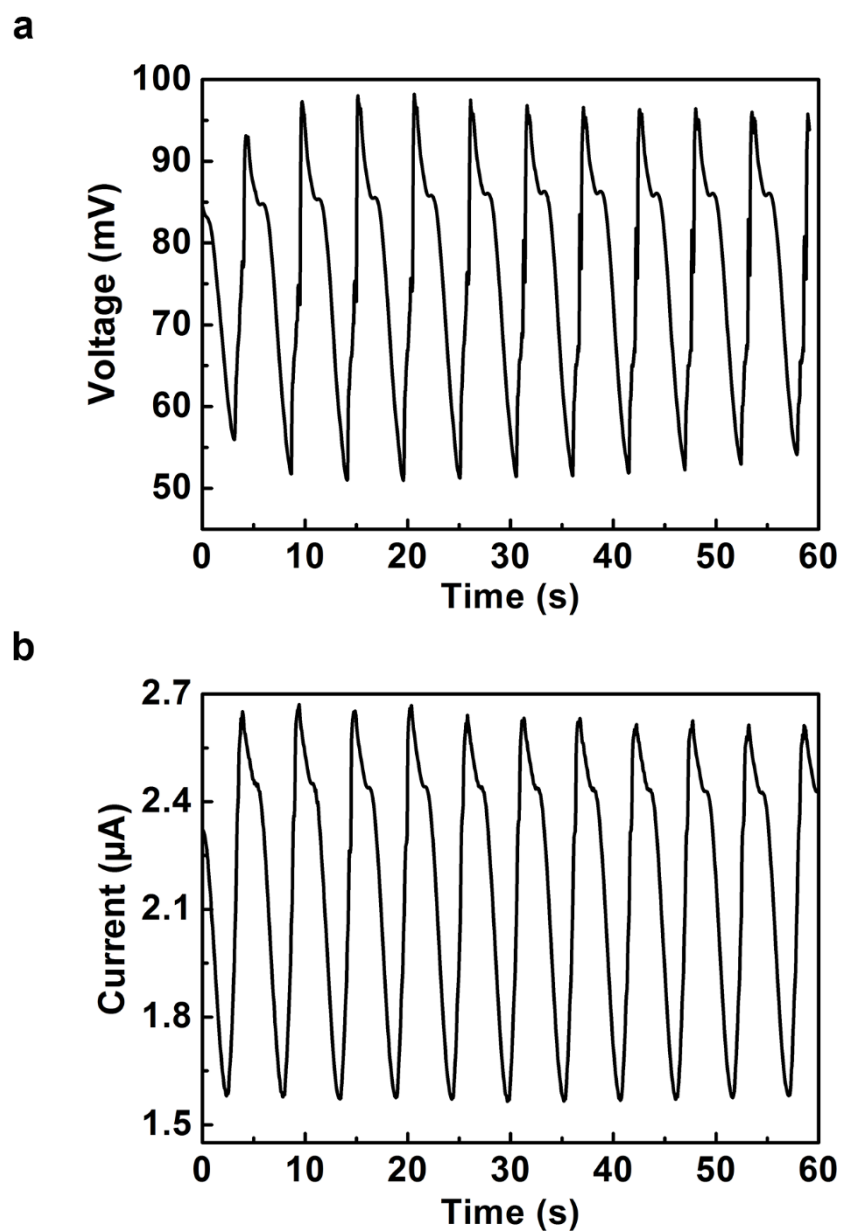


Figure S20. a) and b) Output voltage and current by stretching a 15-cm-long OMC-incorporated FFNG to 150% and releasing in saturated NaCl solution with an immersed length of 2.5 cm. The stretching frequency and velocity were 0.17 Hz and 2.7 cm/s, respectively.

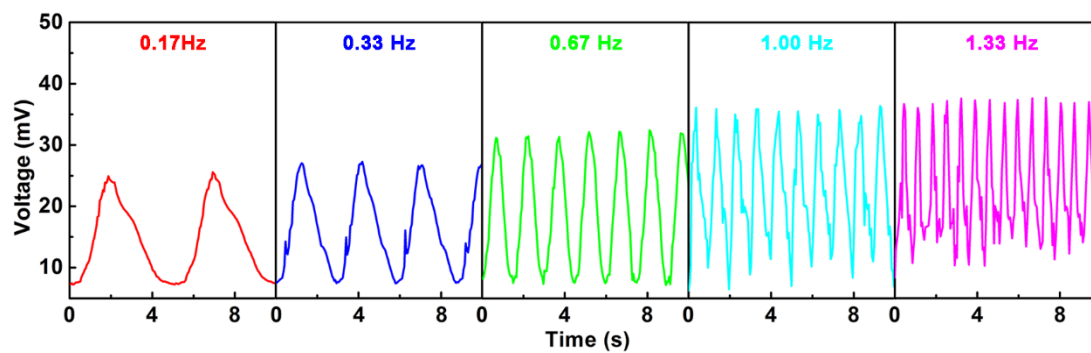


Figure S21. Output voltages at increasing frequencies by stretching the elastic FFNG to 180% and releasing in saturated NaCl solution with the same immersed length of 5.0 cm. The FFNG length was 10 cm.

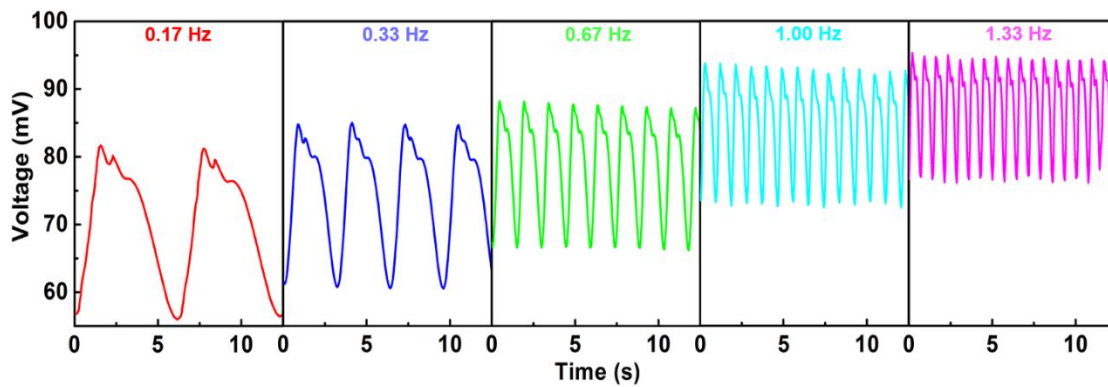


Figure S22. Output voltages at increasing frequencies by stretching the elastic OMC-incorporated FFNG to 180% and releasing in saturated NaCl solution with the same immersed length of 2.5 cm. The FFNG length was 10 cm, and the OMC content was 5.1 $\mu\text{g}/\text{cm}$.

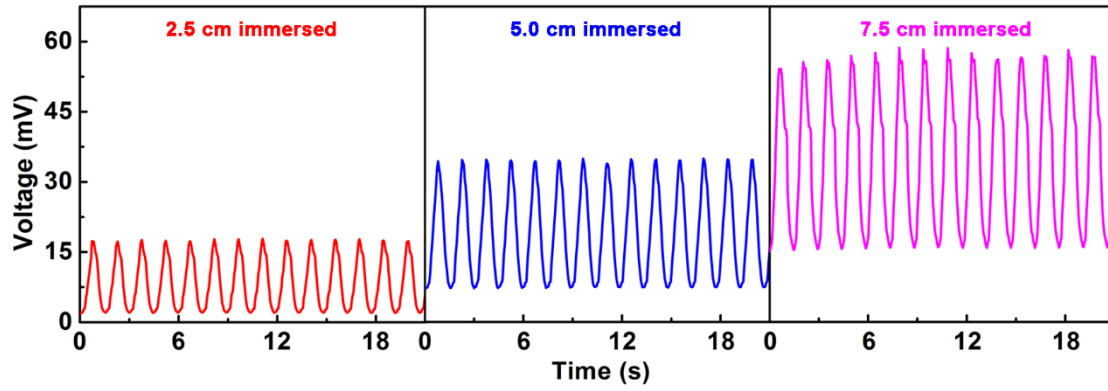


Figure S23. Output voltages at increasing immersed lengths by stretching the elastic FFNG to 180% and releasing in saturated NaCl solution under the same stretching frequency of 0.67 Hz. The FFNG length was 10 cm.

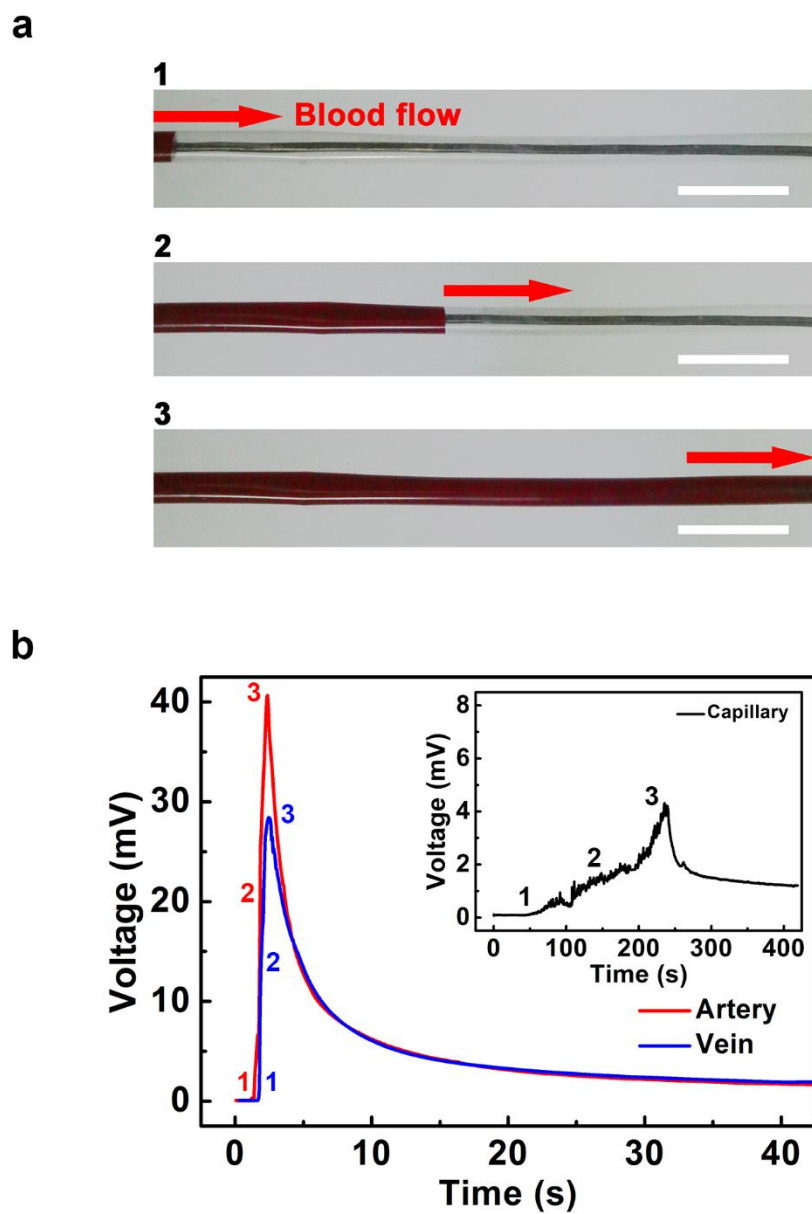


Figure S24. **a)** Photographs of the blood flowing over the FFNG. Scale bar, 1 cm. **b)** Output voltages in the flowing blood at different velocities corresponding to those in artery, vein and capillary (inset). The number of 1, 2 or 3 corresponds to a specific flowing process.

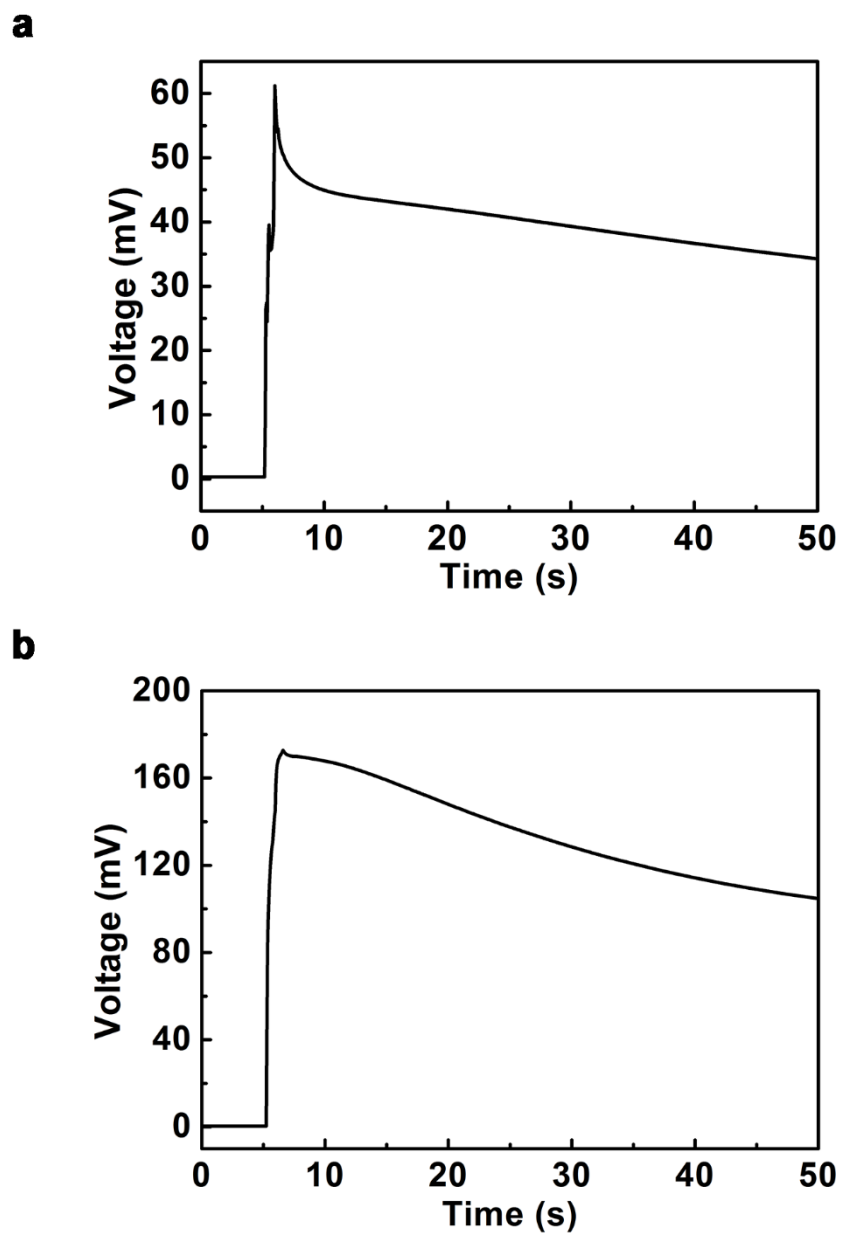


Figure S25. a) and b) Output voltages of an OMC-incorporated FFNG by flowing 0.01 M and 0.1 M PBS solutions, respectively.

Zeta Potential Distribution

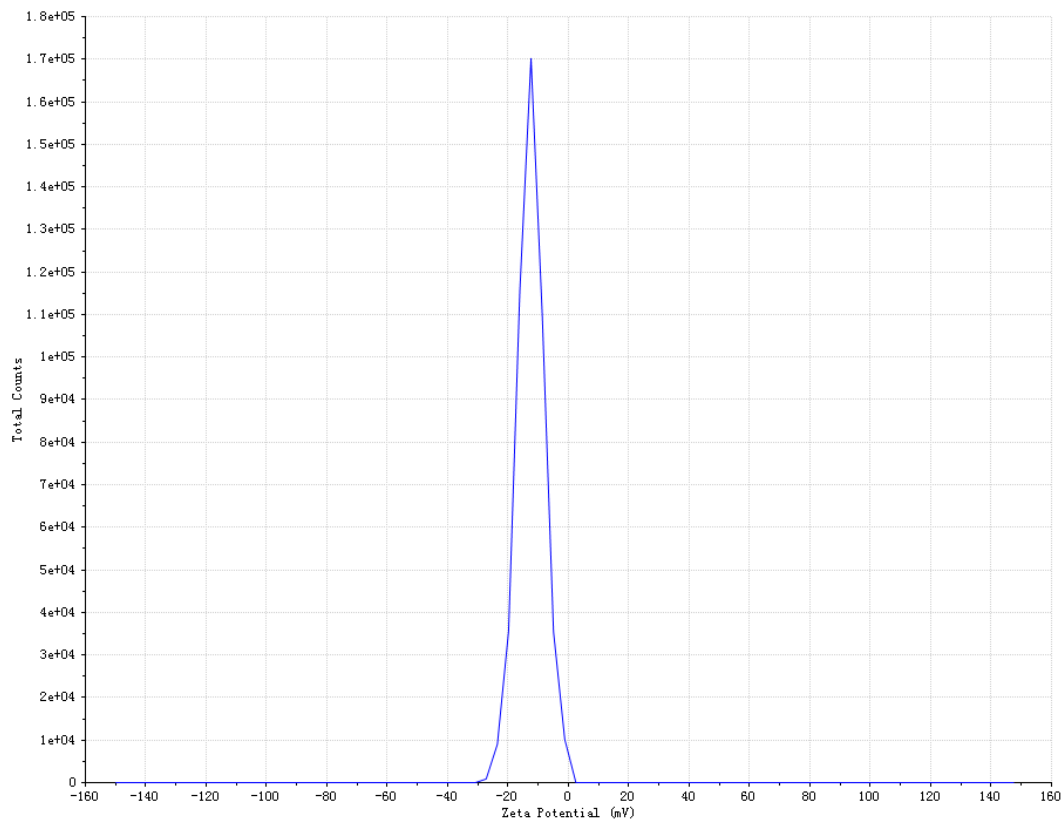


Figure S26. Zeta potential of the CNT in deionized water.

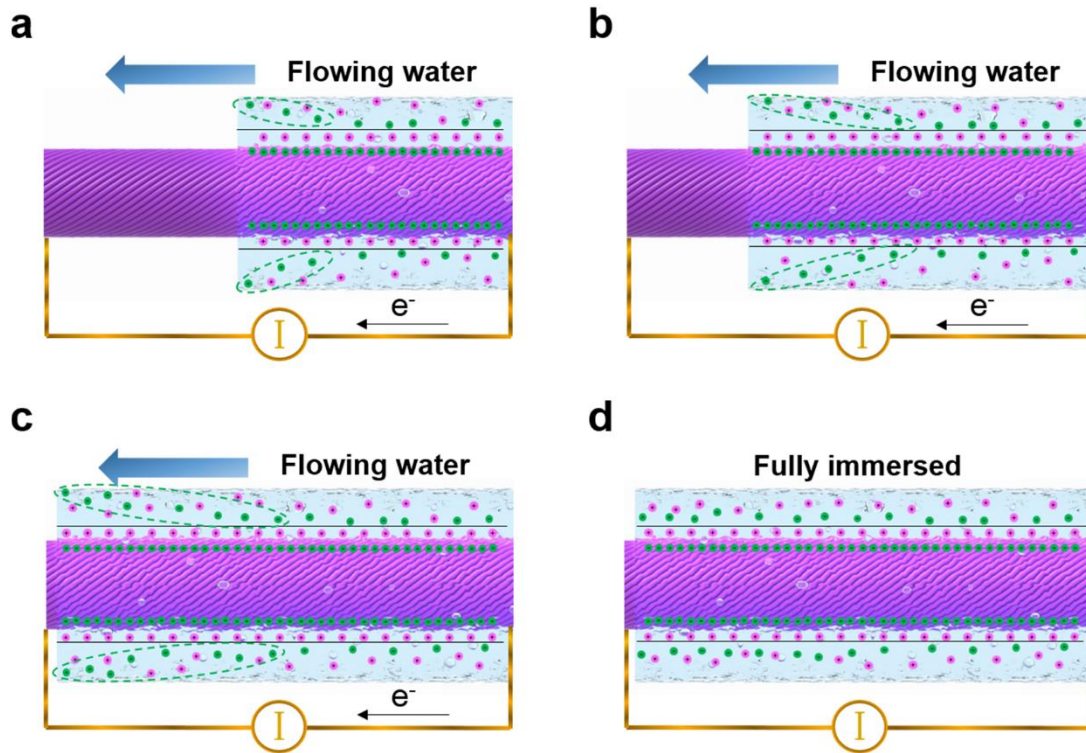


Figure S27. Schematic illustration to the flowing process of saline water and the EDL built on the surface of the FFNG. The purple and green dots represent the positive and negative charges, respectively. The flowing process caused the unbalanced charge between the anions and cations at the front end of the FFNG immersed, as the anions are more retarded in migration to form the diffusion layer and counteract the net charge of the stern layer. After being fully immersed, the net charge of the cations could be eventually screened by the anions.

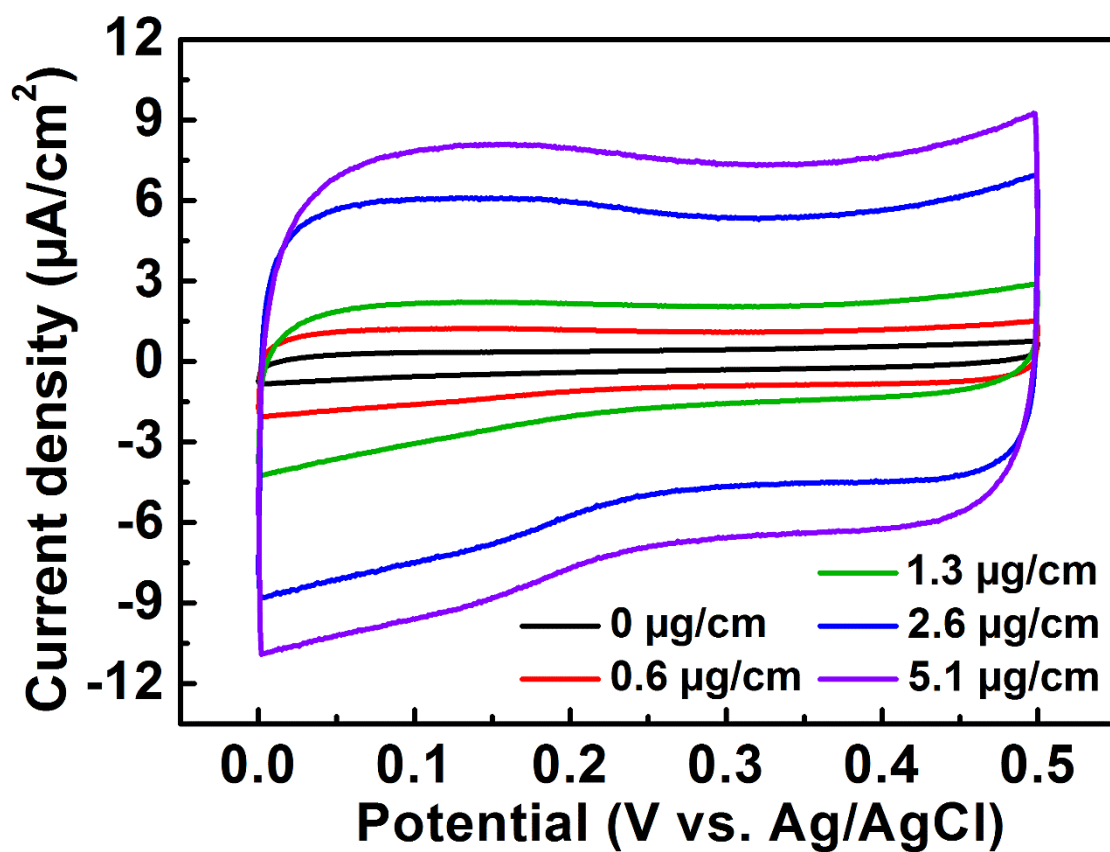


Figure S28. Cyclic voltammograms of the FFNG with increasing OMC contents. They were measured in a saturated NaCl solution with platinum as the counter electrode at a scan rate of 50 mV/s.

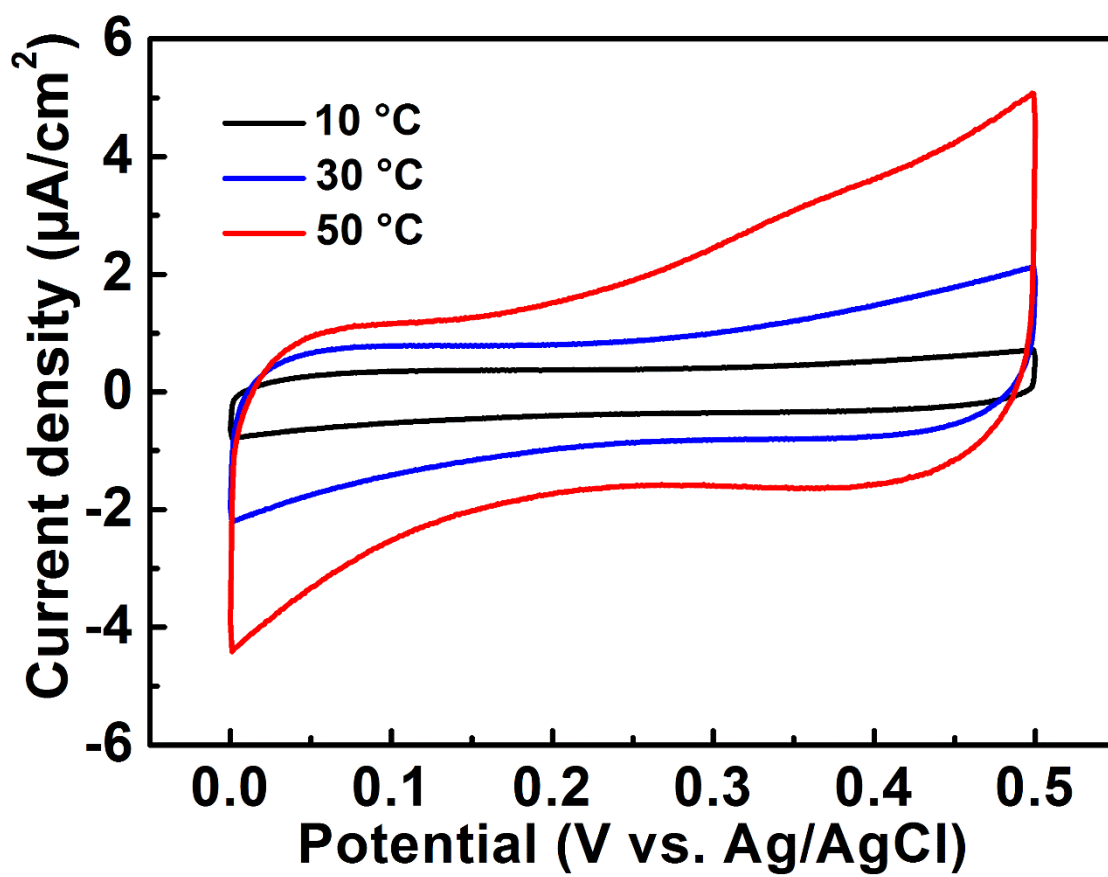


Figure S29. Cyclic voltammograms of the FFNG measured in a 0.6 M NaCl solution with increasing solution temperatures. They were measured at a scan rate of 50 mV/s with the use of platinum counter electrode.

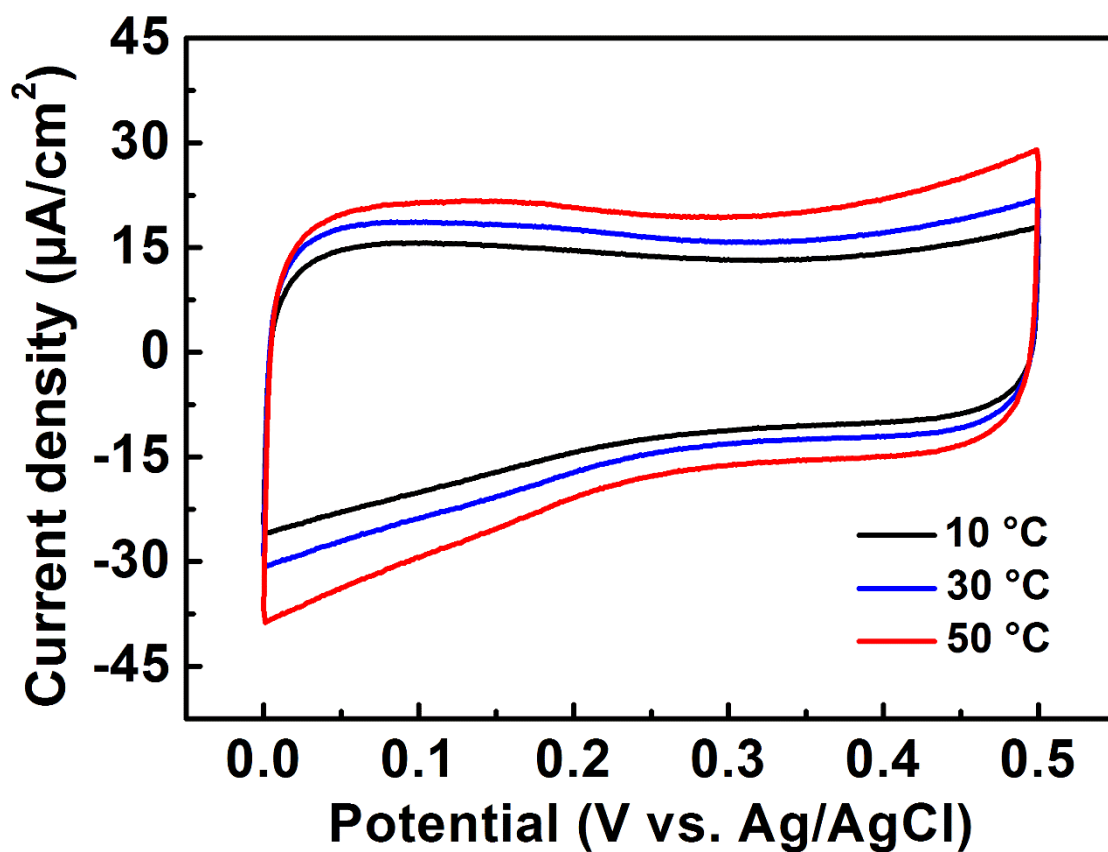


Figure S30. Cyclic voltammograms of the OMC-incorporated FFNG measured in a 0.6 M NaCl solution with increasing solution temperatures. They were measured at a scan rate of 50 mV/s with the use of platinum counter electrode.

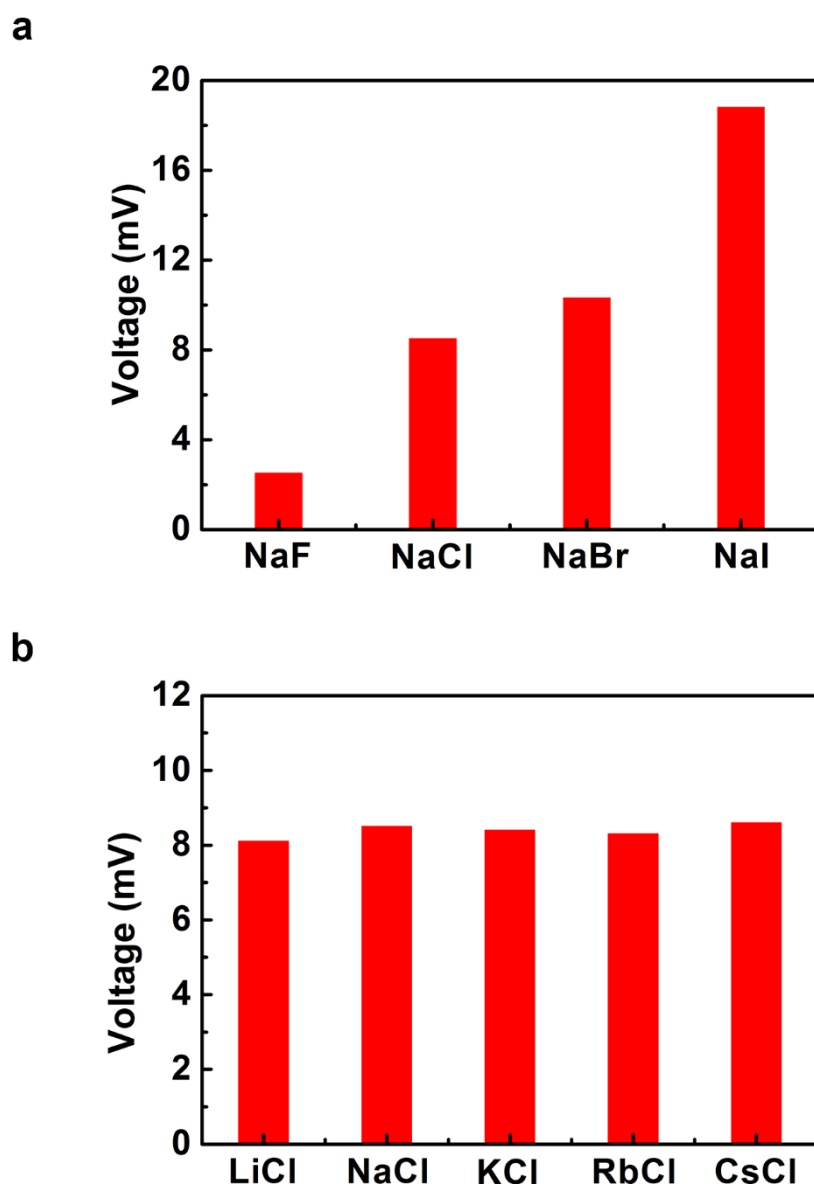


Figure S31. a) Output voltages by dipping the FFNG into LiCl, NaCl, KCl, RbCl and CsCl solutions. b) Output voltages by dipping the FFNG into NaF, NaCl, NaBr and NaI solutions. The FFNG length was 10 cm, the immersed length was 6 cm, the concentration of the solution was 0.6 M, and the dipping velocity was 16 cm/s.

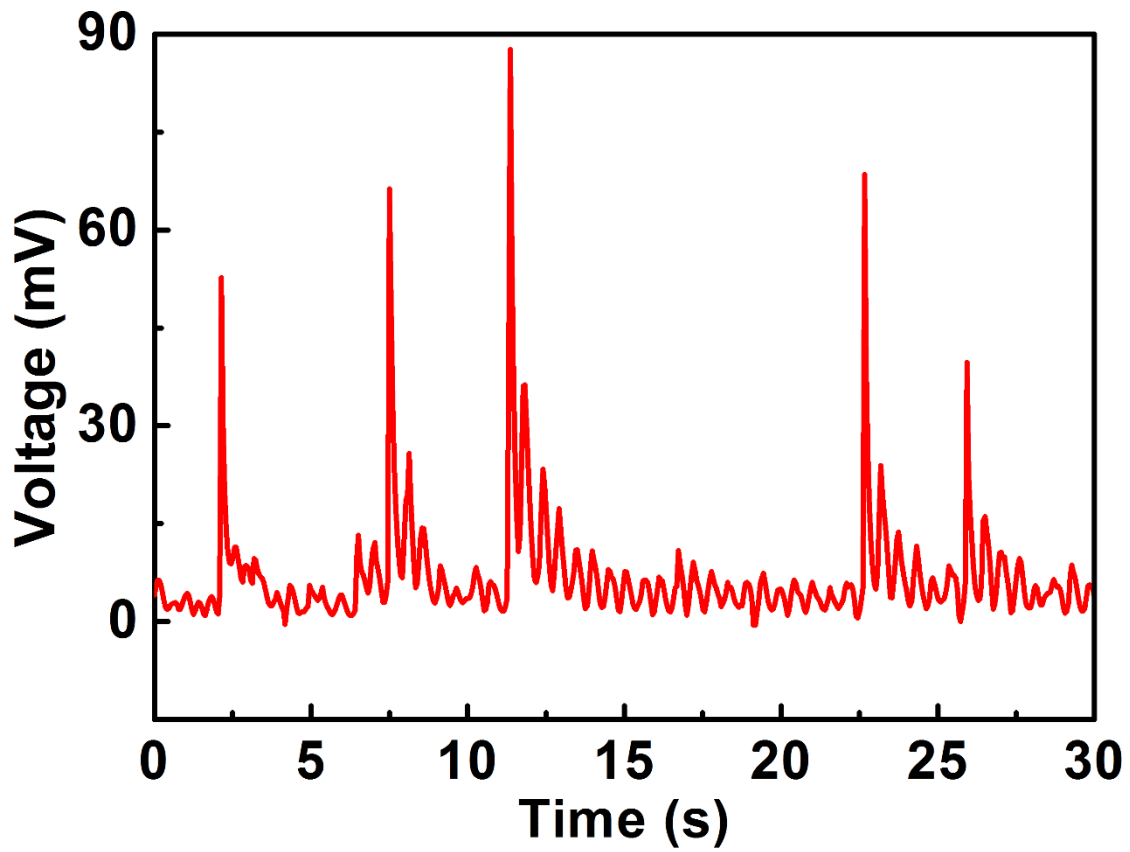


Figure S32. Output voltages produced by the FFNG half immersed in sea water. The voltage peak was generated through the wave.

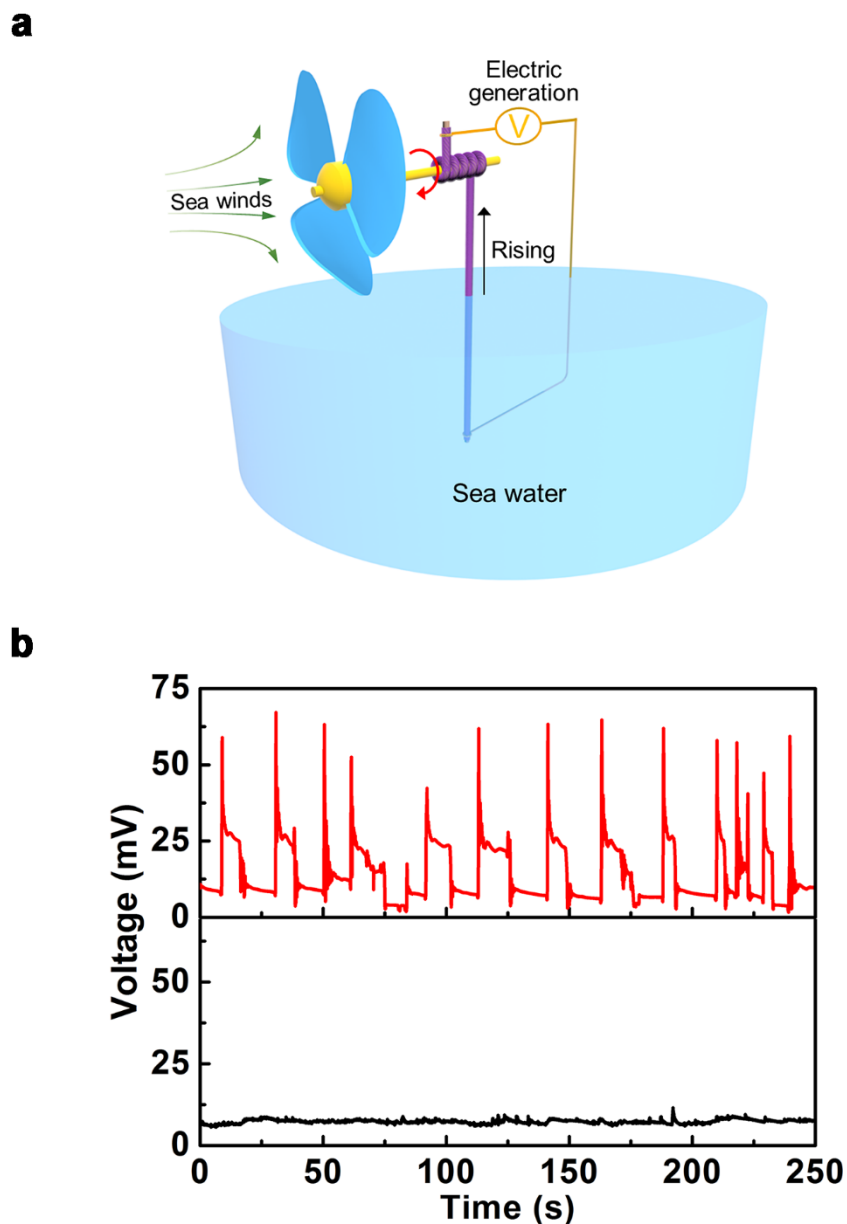


Figure S33. a) Schematic illustration to harvest wind energy by the FFNG. It was tied to the axis of a fan to sense the natural wind. The fan rotation caused the FFNG to move back and forth to produce voltage signals. **b)** Output voltages generated from natural wind (top graph) and windless condition (bottom graph).

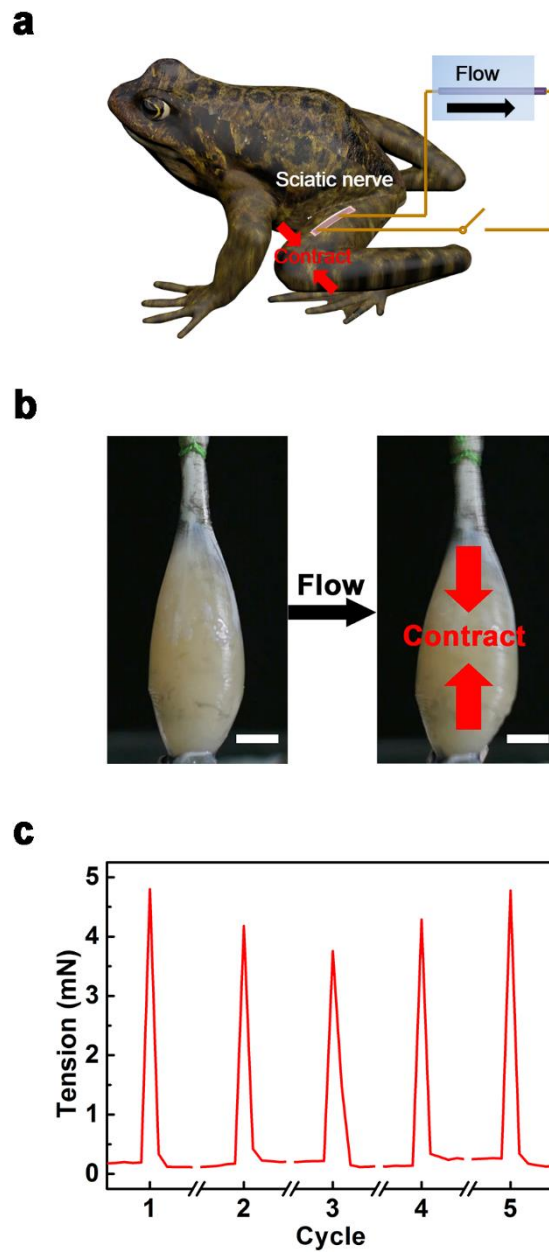


Figure S34. **a)** Schematic illustration to the FFNG connected to the sciatic nerve of a frog to stimulate the gastrocnemius muscle with flowing potential. **b)** Photograph of the gastrocnemius muscle showing contraction simulated by the FFNG in flowing PBS solution. A force sensor was tied to the muscle to detect the contraction force. Scale bar, 0.5 cm. **c)** Continuous tension generation by stimulating the sciatic nerve.

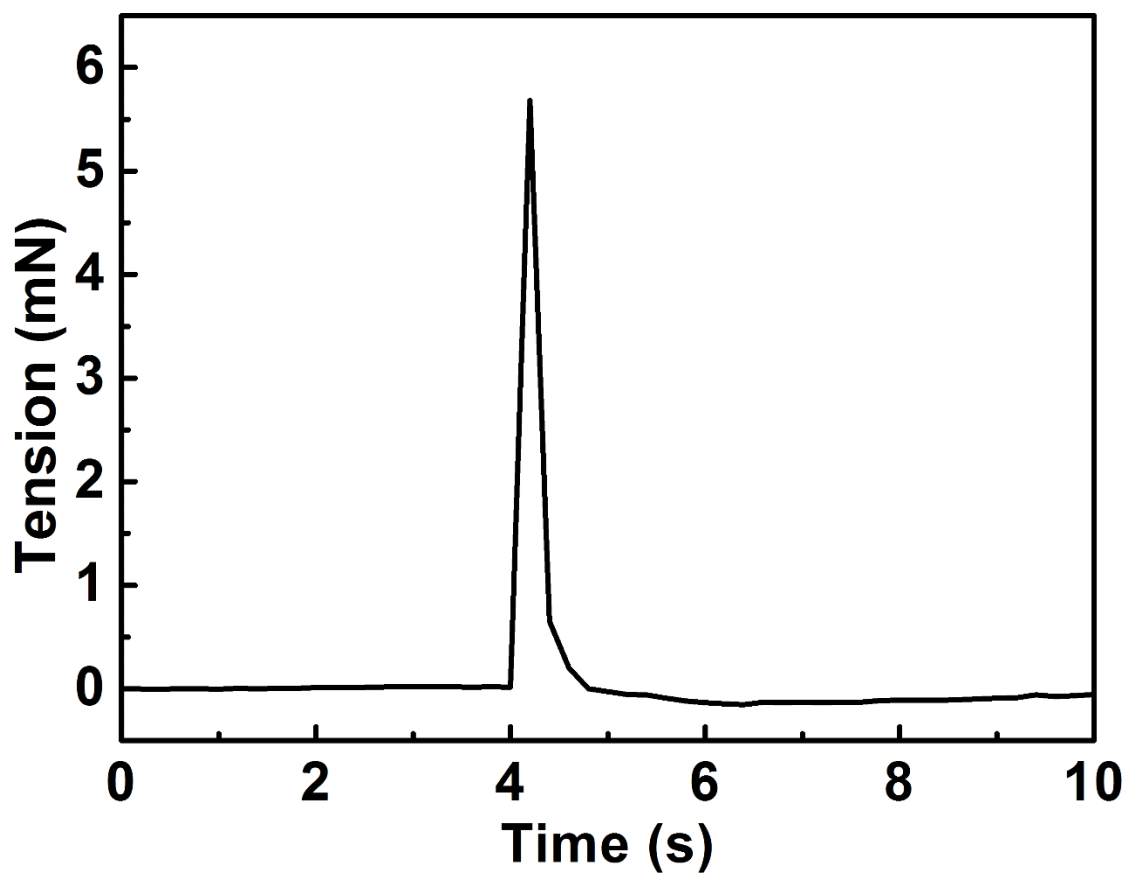


Figure S35. Contraction force generated by the PBS-flow-induced potential of the FFNG. The OMC content on the FFNG was 5.1 $\mu\text{g}/\text{cm}$.

Caption for Supporting Movie

Movie S1. An FFNG was deformed for up to 1,000,000 cycles in NaCl solution. The FFNG had been attached to a motor.

Supporting References

- [1] R. Que, M. Shao, S. Wang, D. D. D. Ma, S.-T. Lee, *Nano Lett.* **2011**, *11*, 4870-4873.
- [2] Y. Yang, K. C. Pradel, Q. Jing, J. M. Wu, F. Zhang, Y. Zhou, Y. Zhang, Z. L. Wang, *ACS Nano* **2012**, *6*, 6984-6989.
- [3] G. Zhu, Y. Su, P. Bai, J. Chen, Q. Jing, W. Yang, Z. L. Wang, *ACS Nano* **2014**, *8*, 6031-6037.